

# Active RIS-Aided Massive MIMO With Imperfect CSI and Phase Noise

Zhangjie Peng, Jianchen Zhu, Cunhua Pan, *Senior Member, IEEE*, Zaichen Zhang, *Senior Member, IEEE*, Daniel Benevides da Costa, *Senior Member, IEEE*, Maged ElKashlan, *Senior Member, IEEE*, and George K. Karagiannidis, *Fellow, IEEE*

**Abstract**—Active reconfigurable intelligent surface (RIS) has attracted significant attention as a recently proposed RIS architecture. Owing to its capability to amplify the incident signals, active RIS can mitigate the multiplicative fading effect inherent in the passive RIS-aided system. In this paper, we consider an active RIS-aided uplink multi-user massive multiple-input multiple-output (MIMO) system in the presence of phase noise at the active RIS. Specifically, we employ a two-timescale scheme, where the beamforming at the base station (BS) is adjusted based on the instantaneous aggregated channel state information (CSI) and the statistical CSI serves as the basis for designing the phase shifts at the active RIS, so that the feedback overhead and computational complexity can be significantly reduced. The aggregated channel composed of the cascaded and direct channels is estimated by utilizing the linear minimum mean square error (LMMSE) technique. Based on the estimated channel, we derive the analytical closed-form expression of a lower bound of the achievable rate. The power scaling laws in the active RIS-aided system are investigated based on the theoretical expressions. When the transmit power of each user is scaled down by the number of BS antennas  $M$  or reflecting elements  $N$ , we find that the thermal noise will cause the lower bound of the achievable rate to approach zero, as the number of  $M$  or  $N$  increases to infinity. Moreover, an optimization approach based on genetic algorithms (GA) is introduced to tackle the phase shift optimization problem. Numerical results reveal that the active RIS can greatly enhance the performance of the considered system under various settings.

**Index Terms**—Reconfigurable intelligent surface (RIS), active RIS, massive MIMO, phase noise, imperfect CSI.

## I. INTRODUCTION

RECENTLY, the reconfigurable intelligent surface (RIS) sparks considerable attention due to its deployment for attaining superior system performance [1]–[3]. Specifically, the RIS comprises numerous cost-effective and passive reconfigurable elements. These passive elements can intelligently

adjust the phase shifts of the impinging waves by a controller. In addition, the RIS operates without the need for radio frequency (RF) chains and digital signal processing circuits, allowing for a thin construction that facilitates easy installation on building facades and indoor spaces [4].

On the other side, massive multiple-input multiple-output (MIMO) constitutes a technology within fifth generation (5G) communication standards, which allows to serve multiple users simultaneously by spatial multiplexing [5]. With a considerable number of antennas deployed at the base station (BS), the massive MIMO system can achieve performance enhancement [6]. Based on the aforementioned benefits of RISs, the combination of massive MIMO systems and RISs presents a compelling solution for future communication needs. Hence, the research of RIS-aided massive MIMO communication systems has drawn significant attention from academia and industry. In [7], unmanned aerial vehicles are integrated into the RIS-aided massive MIMO system, extending the network coverage. The authors of [8] demonstrated that deploying the RIS into the massive MIMO system can achieve great improvements in spectral efficiency by jointly optimizing the active and passive beamforming. Moreover, an alternating optimization framework was proposed in [9], maximizing channel capacity through joint passive beamforming and antenna selection in RIS-aided massive MIMO systems.

In order to leverage the advantages offered by these additional antennas, the channel state information (CSI) is necessary for the operation of communication systems. However, previous works only considered designing the phase shifts of the RIS based on instantaneous CSI, and such scheme brings two challenges. Specifically, one is that the overhead of obtaining instantaneous CSI is prohibitively high in RIS-aided massive MIMO systems given the large amount of reflecting elements [10]. The other concerns the calculation of the optimal beamforming coefficients of the RIS, which need to be transmitted to the RIS controller via a dedicated feedback link [3]. Due to the dynamic and evolving nature of wireless environments, the information feedback and the beamforming calculation require to be frequently executed, which leads to a high computational complexity and energy consumption in the instantaneous CSI-based scheme. Given the aforementioned drawbacks, a novel approach based on a two-timescale scheme was proposed in [11]–[13]. In particular, the instantaneous CSI of the aggregated channel is independent of the number of RIS elements and it can be used in designing the transmit beamforming at the BS. Besides, the configuration of the RIS

Z. Peng and J. Zhu are with the College of Information, Mechanical and Electrical Engineering, Shanghai Normal University, Shanghai 200234, China (e-mail: pengzhangjie@shnu.edu.cn; 1000526997@smail.shnu.edu.cn).

C. Pan and Z. Zhang are with the National Mobile Communications Research Laboratory, Southeast University, Nanjing 210096, China (e-mail: cpan@seu.edu.cn; zczhang@seu.edu.cn).

D. B. da Costa is with the Department of Electrical Engineering, King Fahd University of Petroleum & Minerals, Dhahran 31261, Saudi Arabia (e-mail: danielbcosta@ieee.org).

M. ElKashlan is with the School of Electronic Engineering and Computer Science, Queen Mary University of London, E1 4NS London, U.K. (e-mail: maged.elkashlan@qmul.ac.uk).

G. K. Karagiannidis is with the Department of Electrical and Computer Engineering, Aristotle University of Thessaloniki, 54124 Thessaloniki, Greece, and also with the Artificial Intelligence & Cyber Systems Research Center, Lebanese American University (LAU), Lebanon (e-mail:geokarag@auth.gr).

phase shifts is dependent upon the long-term statistical CSI which varies slowly and does not require frequent updates in each channel coherence interval. As a result, a reduction in computational complexity and estimation overhead can be obtained by using statistical CSI [14]–[16].

However, implementing the RIS can yield limited performance enhancements due to the “multiplicative fading” or “double fading” effect. As we all know, the signals of the transmitter need to pass through the cascaded channel, i.e., the transmitter-RIS-receiver link in RIS-aided systems. Herein, the equivalent path-loss of the cascaded link is treated as a product of the path-loss of the links at both ends of the RIS. This leads to the path-loss of the cascaded link being comparatively larger than that of the direct link [17]. Therefore, the received signals are vulnerable to the multiplicative fading effect.

To overcome the limitations on the potential of traditional passive RISs, the authors of [18] introduced a novel RIS architecture, named active RIS, where an active reflection-type amplifier is integrated into each RIS element. While retaining the ability to adjust phase shifts like passive RISs, the significant capability of active RISs lies in amplifying the incident signals. This new RIS architecture offers a promising solution to counteract multiplicative fading effect. Consequently, there has been a surge of research contributions in the literature. The authors of [19] studied the secure transmission in an active RIS-aided multi-antenna system. In [20], a comparison between the active RIS-aided single-input single-output (SISO) system and the passive counterpart was conducted under the same power budget. The authors of [21] investigated the energy efficiency of active RIS-aided multi-user multiple-input single-output (MU-MISO) systems.

However, an unavoidable problem in active RIS-aided systems has been overlooked by all of the aforementioned works: the phase noise arising from imperfect configuration of the phase shifts at the RIS. Hence, it is imperative to account for the phase noise present at the RIS in practical RIS-aided systems. In [22], the performance degradation induced by the phase noise at the active RIS was demonstrated in the active RIS-aided SISO system. The authors of [23] derived the approximate closed-form expression of the ergodic sum rate of an active RIS-aided multi-pair device-to-device system with phase noise. However, research on integrating the active RIS into the massive MIMO system while taking the phase noise at the RIS into account remains largely unexplored.

Against the aforementioned backgrounds, we focus on an active RIS-aided uplink massive MIMO wireless communication system in the presence of imperfect CSI and phase noise at the active RIS. In contrast to prior research [19]–[23], we take into account a substantial number of antennas deployed at the BS, which is a more complex scenario to adapt for the future communications. Besides, we adopt the two time-scale scheme in the considered system to reduce the channel estimation overhead, feedback overhead and the computational complexity considering the significant quantity of BS antennas and reflecting elements. The main contributions can be outlined as follows:

- We investigate an active RIS-aided uplink massive MIMO wireless communication system considering the phase

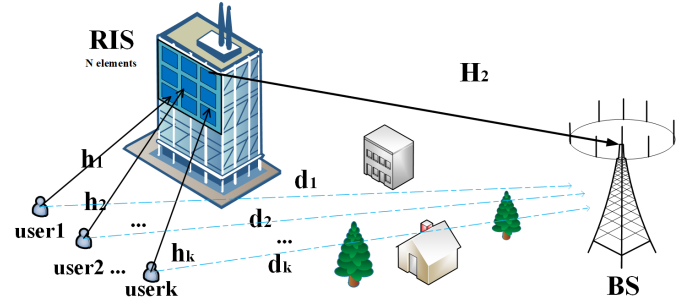


Fig. 1. An active RIS-aided uplink communication system.

noise at the active RIS and the direct links between the users and the BS.

- With imperfect CSI, we employ a linear minimum mean square error (LMMSE) algorithm for estimating the aggregated channel including the cascaded and direct links. Based on the estimated aggregated channel, the maximum ratio combining (MRC) technique is adopted to the received signals at the BS.
- We obtain the closed-form expressions dependent on statistical CSI for the lower bound of the achievable rate in the active RIS-aided massive MIMO system. Then, the power scaling laws of the considered system in different scenarios are analyzed to obtain meaningful conclusions.
- To guarantee fairness among multiple users, we address the problem of maximizing the minimum user rate by utilizing a genetic algorithm (GA). Simulation results reveal that the active RIS can significantly enhance the system performance.

The remainder of this paper is structured as follows. Section II describes the system model of an active RIS-aided massive MIMO system. In Section III, we perform the derivation and analysis of channel estimation based on LMMSE. The expression of the UatF bound of the achievable rate and analysis of the corresponding power scaling laws are included in Section IV. In Section V, the optimization problem for maximizing the minimum user rate is resolved based on a GA. Section VI provides the numerical results. Section VII presents a brief conclusion.

*Notations:* Vectors and matrices are represented by lowercase and uppercase symbols, respectively. The inverse, transpose and conjugate transpose of a matrix are represented by  $(\cdot)^{-1}$ ,  $(\cdot)^T$  and  $(\cdot)^H$ , respectively. Furthermore, we use  $\mathbb{E}\{\cdot\}$ ,  $\text{Tr}\{\cdot\}$  and  $\text{Re}\{\cdot\}$  to represent the expectation, trace and the real part of a complex number, respectively. Also,  $\text{diag}(\mathbf{X})$  denotes a diagonal matrix composed of elements from the diagonal of  $\mathbf{X}$ .  $|\cdot|$  and  $\|\cdot\|$  denote the absolute value of a complex number and the norm of a vector, respectively.  $\mathbf{I}_M$  denotes a  $M \times M$  identity matrix. A vector denoted by  $\mathcal{CN}(0, \Sigma)$  follows a circularly symmetric complex Gaussian distribution, with zero mean and a covariance matrix  $\Sigma$ .

## II. SYSTEM MODEL

Our focus lies on the uplink transmission of an active RIS-aided massive MIMO system which is illustrated in Fig. 1.

Specifically, there are  $K$  single-antenna users near the active RIS communicating with a BS. In this system, the active RIS comprises  $N$  reflecting elements and the BS is equipped with  $M$  antennas. Moreover, there are also direct links from the users to the BS.

As depicted in Fig. 1, the direct link from user  $k$  to the BS, the channel from user  $k$  to the active RIS, and the channel from the active RIS to the BS are denoted by  $\mathbf{d}_k \in \mathbb{C}^{M \times 1}$ ,  $\mathbf{h}_k \in \mathbb{C}^{N \times 1}$  and  $\mathbf{H}_2 \in \mathbb{C}^{M \times N}$ , respectively. Also, the phase shift matrix of the active RIS is represented by  $\Phi = \text{diag}\{e^{j\theta_1}, \dots, e^{j\theta_N}\} \in \mathbb{C}^{N \times N}$ , where  $\theta_n$  denotes the phase shift of the  $n$ -th reflection unit within the interval  $[0, 2\pi)$ . The reflection coefficient matrix of the active RIS is given by  $\mathbf{A} = \text{diag}\{\eta_1, \dots, \eta_N\} \in \mathbb{C}^{N \times N}$ , where  $\eta_n$  denotes the amplification factor of the  $n$ -th RIS element, and its value can surpass one due to the amplifiers of the active RIS. For the simplification of subsequent research, we assume that  $\eta_n = \eta$ .

Given the physical positions of the RIS and the BS in Fig. 1, we employ the Rician fading model to characterize the user-RIS channel and the RIS-BS channel respectively as follows

$$\mathbf{h}_k = \sqrt{\frac{\alpha_k}{\varepsilon_k + 1}} \left( \sqrt{\varepsilon_k} \bar{\mathbf{h}}_k + \tilde{\mathbf{h}}_k \right), k \in \mathcal{K}, \quad (1)$$

$$\mathbf{H}_2 = \sqrt{\frac{\beta}{\delta + 1}} \left( \sqrt{\delta} \bar{\mathbf{H}}_2 + \tilde{\mathbf{H}}_2 \right), \quad (2)$$

where  $\alpha_k$  and  $\beta$  are the path-loss coefficients that vary with distance, whereas  $\varepsilon_k$  and  $\delta$  stand for the Rician factors of corresponding paths. Meanwhile, the set of users is denoted by  $\mathcal{K} = \{1, 2, \dots, K\}$ . Moreover,  $\bar{\mathbf{h}}_k$  and  $\bar{\mathbf{H}}_2$  signify the line-of-sight (LoS) components, whereas  $\tilde{\mathbf{h}}_k$  and  $\tilde{\mathbf{H}}_2$  represent the non-LoS (NLoS) components. Specifically, the elements of  $\tilde{\mathbf{h}}_k$  and  $\tilde{\mathbf{H}}_2$  follow independent and identically distributed (i.i.d.) complex Gaussian distributions, each with a mean of zero and a variance of one. In this paper, the BS and the RIS both adopt the uniform square planar arrays (USPA). Therefore, we can express  $\bar{\mathbf{h}}_k$  and  $\bar{\mathbf{H}}_2$  as follows

$$\bar{\mathbf{h}}_k = \mathbf{a}_N(\varphi_{k,r}^a, \varphi_{k,r}^e), k \in \mathcal{K}, \quad (3)$$

$$\bar{\mathbf{H}}_2 = \mathbf{a}_M(\phi_r^a, \phi_r^e) \mathbf{a}_N^H(\varphi_t^a, \varphi_t^e), \quad (4)$$

where  $\varphi_{k,r}^a(\varphi_{k,r}^e)$  is the azimuth (elevation) angle of arrival (AoA) at the RIS from user  $k$ ,  $\varphi_t^a(\varphi_t^e)$  is the azimuth (elevation) angle of departure (AoD) reflected towards the BS by the RIS.  $\phi_r^a(\phi_r^e)$  is the azimuth (elevation) AoA from the RIS to the BS, respectively. Besides, the  $i$ -th entry of the array response vector  $\mathbf{a}_X(\vartheta^a, \vartheta^e) \in \mathbb{C}^{X \times 1}$ ,  $X \in \{M, N\}$ , can be described as

$$[\mathbf{a}_X(\vartheta^a, \vartheta^e)]_i = \exp\left\{j2\pi \frac{d}{\lambda} \left( \left[ (x-1)\sqrt{X} \right] \sin \vartheta^e \sin \vartheta^a + \left( (x-1) \bmod \sqrt{X} \right) \cos \vartheta^e \right) \right\}, \quad (5)$$

where  $d$  stands for the antenna or element spacing, with  $\lambda$  representing the wavelength. Furthermore, we use  $\mathbf{a}_M$  and  $\mathbf{a}_N$  to simplify the representation of  $\mathbf{a}_M(\phi_r^a, \phi_r^e)$  and  $\mathbf{a}_N(\varphi_t^a, \varphi_t^e)$  respectively.

Considering the presence of various obstructions like trees and buildings between the users and the BS, the direct link between user  $k$  and the BS experiences Rayleigh fading, which is depicted as

$$\mathbf{d}_k = \sqrt{\gamma_k} \tilde{\mathbf{d}}_k, k \in \mathcal{K}, \quad (6)$$

where  $\gamma_k$  is the large-scale path-loss factor. The entries of

$\tilde{\mathbf{d}}_k$  are i.i.d. complex Gaussian random variables, i.e.,  $\tilde{\mathbf{d}}_k \sim \mathcal{CN}(0, \mathbf{I}_M)$ .

Herein, we consider the imperfect hardware at the active RIS. Specifically, given the inherent limitations in configuring the reflection phases of RIS with limited precision, they can be characterized as phase noise [24]. Therefore, the hardware impairment at the active RIS is described in a random diagonal matrix comprised of  $N$  random phase noise [25], and we have

$$\Theta = \text{diag}\left\{e^{j\tilde{\theta}_1}, e^{j\tilde{\theta}_2}, \dots, e^{j\tilde{\theta}_N}\right\} \in \mathbb{C}^{N \times N}. \quad (7)$$

In (7),  $\tilde{\theta}_n$  follows a Von Mises distribution with a mean of zero whose probability density function (PDF) is  $M_v(\tilde{\theta}) = \frac{e^{v \cos(\tilde{\theta})}}{2\pi I_0(v)}$ , with the concentration parameter  $v$ . The characteristic function of  $\tilde{\theta}$  can be obtained as  $E\{e^{j\tilde{\theta}}\} = \frac{I_1(v)}{I_0(v)} \triangleq \rho$ ,  $E\{e^{j2\tilde{\theta}}\} = \frac{I_2(v)}{I_0(v)} \triangleq l$ , where  $I_n(v)$  represents the modified Bessel function of the first kind and  $n$  represents its order.

Considering the phase noise at the RIS in transmission, we can obtain the cascaded user-RIS-BS channel as  $\mathbf{G} = [\mathbf{g}_1, \mathbf{g}_2, \dots, \mathbf{g}_K] = \mathbf{H}_2 \mathbf{A} \Phi \Theta \mathbf{H}_1 \in \mathbb{C}^{M \times K}$  with  $\mathbf{g}_k = \mathbf{H}_2 \mathbf{A} \Phi \Theta \mathbf{h}_k$ , where  $\mathbf{H}_1 = [\mathbf{h}_1, \mathbf{h}_2, \dots, \mathbf{h}_K]$ . As a result, the aggregated channel from user  $k$  to the BS can be expressed as

$$\begin{aligned} \mathbf{q}_k &= \mathbf{g}_k + \mathbf{d}_k = \mathbf{H}_2 \mathbf{A} \Phi \Theta \mathbf{h}_k + \mathbf{d}_k \\ &= \underbrace{\sqrt{c_k \delta \varepsilon_k} \bar{\mathbf{H}}_2 \mathbf{A} \Phi \Theta \bar{\mathbf{h}}_k}_{\mathbf{q}_k^1} + \underbrace{\sqrt{c_k \delta} \tilde{\mathbf{H}}_2 \mathbf{A} \Phi \Theta \tilde{\mathbf{h}}_k}_{\mathbf{q}_k^2} \\ &\quad + \underbrace{\sqrt{c_k \varepsilon_k} \tilde{\mathbf{H}}_2 \mathbf{A} \Phi \Theta \tilde{\mathbf{h}}_k}_{\mathbf{q}_k^3} + \underbrace{\sqrt{c_k} \tilde{\mathbf{H}}_2 \mathbf{A} \Phi \Theta \tilde{\mathbf{h}}_k}_{\mathbf{q}_k^4} + \sqrt{\gamma_k} \tilde{\mathbf{d}}_k, \end{aligned} \quad (8)$$

where  $c_k \triangleq \frac{\beta \alpha_k}{(\delta+1)(\varepsilon_k+1)}$ . We define the first four terms of (8)

as  $\mathbf{q}_k^1 \sim \mathbf{q}_k^4$ , then  $\mathbf{q}_k = \sum_{w=1}^4 \mathbf{q}_k^w + \mathbf{d}_k \triangleq \mathbf{q}_k + \mathbf{d}_k$ . Therefore, the aggregated channel matrix from users to the BS can be signified by  $\mathbf{Q} = \mathbf{G} + \mathbf{D} = [\mathbf{q}_1, \mathbf{q}_2, \dots, \mathbf{q}_K] \in \mathbb{C}^{M \times K}$ , where  $\mathbf{D} = [\mathbf{d}_1, \mathbf{d}_2, \dots, \mathbf{d}_K]$ . Hence, the received signal vector at the BS is formulated as

$$\mathbf{y} = \sqrt{p} \mathbf{Q} \mathbf{x} = \sqrt{p} \sum_{k=1}^K \mathbf{q}_k x_k + \mathbf{H}_2 \mathbf{A} \Phi \Theta \boldsymbol{\nu} + \mathbf{n}, \quad (9)$$

where the transmit power of each user is denoted by  $p$ ,  $\mathbf{x} = [x_1, x_2, \dots, x_K]^T$  contains the transmit signals of all users,  $\boldsymbol{\nu} \sim \mathcal{CN}(0, \sigma_e^2 \mathbf{I}_N)$  represents the thermal noise which is associated with the input noise and the inherent device noise of the active RIS elements [26], and  $\mathbf{n} \sim \mathcal{CN}(0, \sigma^2 \mathbf{I}_M)$  is the static noise at the BS.

### III. CHANNEL ESTIMATION

In this section, we utilize the LMMSE method for obtaining the estimated aggregated channel  $\hat{\mathbf{Q}}$  based on the received pilot signals in a single coherence interval [25]. Each channel coherence interval spans  $\tau_c$  time slots, of which  $\tau$  time slots are utilized for channel estimation. In each channel coherence interval, the transmit pilot sequences from all users are mutually orthogonal and are simultaneously transmitted to the BS. Specifically, the pilot sequence utilized by user  $k$  is denoted as  $\mathbf{s}_k \in \mathbb{C}^{\tau \times 1}$ , then we have  $\mathbf{S} = [\mathbf{s}_1, \mathbf{s}_2, \dots, \mathbf{s}_K]$ , with  $\mathbf{S}^H \mathbf{S} = \mathbf{I}_K$ . As a result, the pilot signals received at the BS can be given by

$$\mathbf{Y}_p = \sqrt{\tau p} \mathbf{Q} \mathbf{S}^H + \mathbf{H}_2 \mathbf{A} \Phi \Theta \mathbf{V} + \mathbf{N}, \quad (10)$$

where  $\mathbf{N} \in \mathbb{C}^{M \times \tau}$  is the complex Gaussian noise matrix whose entries are i.i.d. with zero mean and variance  $\sigma^2$ . In addition,  $\mathbf{V} \in \mathbb{C}^{N \times \tau}$  is the thermal noise matrix where each entry is modeled as a complex Gaussian random variable with a mean of zero and a variance of  $\sigma_e^2$ . To eliminate the interference from other users, we multiply (10) by  $\frac{\mathbf{s}_k}{\sqrt{\tau p}}$  and leverage the orthogonality inherent in the pilot signals, obtaining the observation vector of user  $k$  as below

$$\mathbf{y}_p^k = \frac{\mathbf{s}_k}{\sqrt{\tau p}} \mathbf{Y}_p = \mathbf{q}_k + \frac{\eta}{\sqrt{\tau p}} \mathbf{H}_2 \Phi \Theta \mathbf{V} \mathbf{s}_k + \frac{1}{\sqrt{\tau p}} \mathbf{N} \mathbf{s}_k. \quad (11)$$

Usually, the MMSE criterion can be employed to obtain optimal estimation of the channel for user  $k$ . While the MMSE estimator needs to know the moments of the channel as well as the fact that the channel follows or closely approximates a complex Gaussian distribution. While the cascaded channel  $\mathbf{g}_k$  is the product of two Gaussian variables and a random diagonal with Von Mises distribution in the considered system. At the cost of little performance loss, we adopt the LMMSE estimator due to its independence from the exact channel distributions. Therefore, the LMMSE estimator is utilized to acquire the estimated channel  $\hat{\mathbf{Q}}$ . By adopting MRC processing where the received signal  $\mathbf{y}$  is multiplied by the receive combining vector  $\hat{\mathbf{q}}_k$ , the expression for the  $k$ -th user of the received signal can be formulated as

$$r_k = \hat{\mathbf{q}}_k^H \mathbf{y} = \sqrt{p} \hat{\mathbf{q}}_k^H \mathbf{q}_k x_k + \sqrt{p} \sum_{i=1, i \neq k}^K \hat{\mathbf{q}}_k^H \mathbf{q}_i x_i + \eta \hat{\mathbf{q}}_k^H \mathbf{H}_2 \Phi \Theta \mathbf{v} + \hat{\mathbf{q}}_k^H \mathbf{n}, k \in \mathcal{K}, \quad (12)$$

where  $\hat{\mathbf{q}}_k$  is the  $k$ -th column of  $\hat{\mathbf{Q}}$ . Subsequently, we provide the necessary statistics for  $\hat{\mathbf{q}}_k$  and  $\mathbf{y}_p^k$ .

*Lemma 1:* The mean vectors and covariance matrices required for calculating the LMMSE estimator are expressed as

$$\mathbb{E}\{\mathbf{q}_k\} = \mathbb{E}\{\mathbf{y}_p^k\} = \eta \rho \sqrt{c_k \delta \varepsilon_k} \bar{\mathbf{H}}_2 \Phi \bar{\mathbf{h}}_k, \quad (13)$$

$$\text{Cov}\{\mathbf{q}_k, \mathbf{y}_p^k\} = \text{Cov}\{\mathbf{q}_k, \mathbf{q}_k\} = a_{k1} \mathbf{a}_M \mathbf{a}_M^H + a_{k2} \mathbf{I}_M, \quad (14)$$

$$\text{Cov}\{\mathbf{y}_p^k, \mathbf{y}_p^k\} = m_k \mathbf{a}_M \mathbf{a}_M^H + n_k \mathbf{I}_M, \quad (15)$$

where  $a_{k1} = \Delta c_k \delta \{ (1 - \rho^2) \varepsilon_k + 1 \}$ ,  $a_{k2} = \Delta c_k (\varepsilon_k + 1) + \gamma_k$ ,  $m_k = a_{k1} + \varpi \delta$  and  $n_k = a_{k2} + \frac{\sigma^2}{\tau p} + \varpi$  with  $\varpi = \frac{\Delta \beta \sigma_e^2}{\tau p (\delta + 1)}$ .

*Proof:* See Appendix B. ■

*Theorem 1:* The expression for the LMMSE estimate  $\hat{\mathbf{q}}_k$  and the estimation's NMSE for  $\mathbf{q}_k$  are represented by (16)

$$\hat{\mathbf{q}}_k = \mathbf{A}_k \mathbf{y}_p^k + \mathbf{B}_k = \underbrace{\eta \sqrt{c_k \delta \varepsilon_k} \mathbf{A}_k \bar{\mathbf{H}}_2 \Phi \Theta \bar{\mathbf{h}}_k}_{\hat{\mathbf{q}}_k^1} + \underbrace{\eta \sqrt{c_k \delta} \mathbf{A}_k \bar{\mathbf{H}}_2 \Phi \Theta \tilde{\mathbf{h}}_k}_{\hat{\mathbf{q}}_k^2} + \underbrace{\eta \sqrt{c_k \varepsilon_k} \mathbf{A}_k \tilde{\mathbf{H}}_2 \Phi \Theta \bar{\mathbf{h}}_k}_{\hat{\mathbf{q}}_k^3} + \underbrace{\eta \sqrt{c_k} \mathbf{A}_k \tilde{\mathbf{H}}_2 \Phi \Theta \tilde{\mathbf{h}}_k}_{\hat{\mathbf{q}}_k^4} + \underbrace{\eta \rho \sqrt{c_k \delta \varepsilon_k} \bar{\mathbf{H}}_2 \Phi \bar{\mathbf{h}}_k}_{\hat{\mathbf{q}}_k^5} - \underbrace{\eta \rho \sqrt{c_k \delta \varepsilon_k} \mathbf{A}_k \bar{\mathbf{H}}_2 \Phi \bar{\mathbf{h}}_k}_{\hat{\mathbf{q}}_k^6} + \frac{\eta}{\sqrt{\tau p}} \mathbf{A}_k \mathbf{H}_2 \Phi \Theta \mathbf{V} \mathbf{s}_k + \frac{1}{\sqrt{\tau p}} \mathbf{A}_k \mathbf{N} \mathbf{s}_k + \sqrt{\gamma_k} \mathbf{A}_k \tilde{\mathbf{d}}_k, \quad (16)$$

$$\text{NMSE}_k = \frac{\text{Tr}\{\mathbf{MSE}_k\}}{\text{Tr}\{\text{Cov}\{\mathbf{q}_k, \mathbf{q}_k\}\}} = \frac{\left(\frac{\sigma^2}{\tau p} + \varpi + M \varpi \delta\right) \left(\frac{\sigma^2}{\tau p} + \varpi\right) (a_{k1} + a_{k2}) + (\varpi \delta + \frac{\sigma^2}{\tau p} + \varpi) (a_{k2}^2 + M a_{k1} a_{k2})}{(a_{k2} + \frac{\sigma^2}{\tau p} + \varpi) \left\{ (a_{k2} + \frac{\sigma^2}{\tau p} + \varpi) + M (a_{k1} + \varpi \delta) \right\} (a_{k1} + a_{k2})}, \quad (17)$$

and (17) respectively at the bottom of this page, where

$$\mathbf{A}_k = \mathbf{A}_k^H = a_{k3} \mathbf{a}_M \mathbf{a}_M^H + a_{k4} \mathbf{I}_M, \quad (18)$$

$$\mathbf{B}_k = (\mathbf{I}_M - \mathbf{A}_k) \eta \sqrt{c_k \delta \varepsilon_k} \bar{\mathbf{H}}_2 \Phi \bar{\mathbf{h}}_k, \quad (19)$$

$$a_{k3} = \frac{\left(\frac{\sigma^2}{\tau p} + \varpi\right) a_{k1} - \varpi \delta a_{k2}}{\left(a_{k2} + \frac{\sigma^2}{\tau p} + \varpi\right)^2 + M (a_{k1} + \varpi \delta) \left(a_{k2} + \frac{\sigma^2}{\tau p} + \varpi\right)}, \quad (20)$$

$$a_{k4} = \frac{a_{k2}}{a_{k2} + \frac{\sigma^2}{\tau p} + \varpi}. \quad (21)$$

*Proof:* See Appendix C. ■

In detail, the first six terms of  $\hat{\mathbf{q}}_k$  are represented by  $\hat{\mathbf{q}}_k^1 \sim \hat{\mathbf{q}}_k^6$  respectively, and we define  $\hat{\mathbf{q}}_k = \sum_{w=1}^6 \hat{\mathbf{q}}_k^w$  for the subsequent calculations. Meanwhile, we find that the phase noise does not manifest within (17), suggesting that the NMSE remains unaffected by the phase noise. Following this, we will explore some insights related to the NMSE.

*Corollary 1:* In the regime of both low and high pilot power-to-noise ratio, the asymptotic behaviors of NMSE are respectively formulated as

$$\lim_{\frac{\sigma^2}{\tau p}, \frac{\sigma_e^2}{\tau p} \rightarrow \infty} \text{NMSE}_k \rightarrow 1, \quad (22)$$

$$\lim_{\frac{\sigma^2}{\tau p}, \frac{\sigma_e^2}{\tau p} \rightarrow 0} \text{NMSE}_k \rightarrow 0. \quad (23)$$

Obviously, the value of NMSE which is between 0 and 1 quantifies the estimation error [27]. As we all know, expanding the quantity of  $N$  can yield a comparable outcome to enlarging the pilot sequence  $\tau$ , leading to a decrease in NMSE within the passive RIS-aided massive MIMO systems. However, this approach proves ineffective for active RIS-aided massive MIMO systems since (17) is independent of  $N$ , which suggests that the demand for reflecting elements in active RIS-aided systems is less critical compared to other systems aiming at enhancing channel estimation quality.

*Corollary 2:* When the RIS-BS channel is the Rayleigh distributed, i.e.,  $\delta = 0$ , we have

$$\text{NMSE}_k = \frac{\frac{\sigma^2}{\tau p} + \Delta \frac{\sigma_e^2 \beta}{\tau p}}{\Delta \beta \alpha_k + \gamma_k + \frac{\sigma^2}{\tau p} + \Delta \frac{\sigma_e^2 \beta}{\tau p}}. \quad (24)$$

*Proof:* As  $\delta = 0$ , we obtain  $a_{k1} = 0$ ,  $a_{k2} = \Delta \beta \alpha_k + \gamma_k$  and  $\varpi = \frac{\Delta \sigma_e^2 \beta}{\tau p}$ . The completion of the proof is achieved by substituting these results into (17). ■

Corollary 2 considers a certain scenario where considerable scatterers exist between the RIS and the BS. We also find the NMSE has a simple analytical expression where it is unaffected by both  $M$  and  $N$ .

#### IV. ANALYSIS OF THE ACHIEVABLE RATE

In this section, we place emphasis on the derivation and analysis of the closed-form expressions for a lower bound of the achievable rate. Then, we investigate the power scaling laws in the system based on the theoretical achievable rate. Additionally, we later substitute ‘‘achievable rate’’ for ‘‘lower bound of the achievable rate’’ to streamline expressions in the content of this paper.

Before embarking on the achievable rate derivation, we first start with the calculation of the amplification factor based on the amplification power  $P_A$ .

*Lemma 2:* The amplification power  $P_A$  can be calculated in a similar manner as [23]

$$P_A = \mathbb{E} \left\{ \left\| \sqrt{p} \mathbf{A} \Phi \Theta \mathbf{H}_1 \mathbf{x} + \mathbf{A} \Phi \Theta \boldsymbol{\nu} \right\|^2 \right\} \\ = \eta^2 N \left( \sum_{k=1}^K p \alpha_k + \sigma_e^2 \right). \quad (25)$$

Although phase noise is present inside  $P_A$ , we observe that it does not have an impact on the amplification power since its characteristic function has not been manifested. Then, given a specific amplification power, we can compute the factor as

$$\eta = \sqrt{\frac{P_A}{N \left( \sum_{k=1}^K p \alpha_k + \sigma_e^2 \right)}} \triangleq \sqrt{\frac{\Delta}{N}}, \quad (26)$$

where  $\Delta = \sqrt{\frac{P_A}{\left( \sum_{k=1}^K p \alpha_k + \sigma_e^2 \right)}}$  for simplicity.

##### A. Derivation of the Rate

For tractable analysis, we take advantage of the use-and-then-forget (UatF) bound as in [27] and [28] to characterize the lower bound of the ergodic rate of the active RIS-aided massive MIMO system. Specifically, by adding and subtracting the term  $\mathbb{E} \{ \hat{\mathbf{q}}_k^H \mathbf{q}_k \} x_k$ , (12) can be reformulated as

$$r_k = \underbrace{\sqrt{p} \mathbb{E} \{ \hat{\mathbf{q}}_k^H \mathbf{q}_k \} x_k}_{\text{Desired signal}} + \underbrace{\sqrt{p} \left( \hat{\mathbf{q}}_k^H \mathbf{q}_k - \sqrt{p} \mathbb{E} \{ \hat{\mathbf{q}}_k^H \mathbf{q}_k \} \right) x_k}_{\text{Signal leakage}} \\ + \underbrace{\sqrt{p} \sum_{i=1, i \neq k}^K \hat{\mathbf{q}}_k^H \mathbf{q}_i x_i}_{\text{Interference}} + \underbrace{\eta \hat{\mathbf{q}}_k^H \mathbf{H}_2 \Phi \Theta \boldsymbol{\nu} + \hat{\mathbf{q}}_k^H \mathbf{n}}_{\text{Noise}}. \quad (27)$$

Afterwards, we get the lower bound of the  $k$ -th user's achievable rate as  $\underline{R}_k = \chi \log_2(1 + \text{SINR}_k)$ , where  $\chi = \frac{\tau_c - \tau}{\tau}$  denotes the factor that characterizes the utilization ratio of slots per coherence block designated for transmission, and the effective SINR $_k$  is presented in (28) at the bottom of this page.

*Theorem 2:* The lower bound for the achievable rate of the  $k$ -th user is expressed as  $\underline{R}_k = \chi \log_2(1 + \text{SINR}_k)$ , and the SINR $_k$  is given by

$$\text{SINR}_k = \frac{p E_k^{\text{signal}}(\Phi)}{p E_k^{\text{leak}}(\Phi) + p \sum_{i=1, i \neq k}^K I_{ki}(\Phi) + E_k^{\text{noise}}(\Phi)}, \quad (29)$$

where the specific expressions of  $E_k^{\text{noise}}(\Phi)$ ,  $E_k^{\text{signal}}(\Phi)$ ,  $I_{ki}(\Phi)$  and  $E_k^{\text{leak}}(\Phi)$  are expressed as (88), (90), (109) and (116) respectively in Appendix D.

*Proof:* See Appendix D.  $\blacksquare$

It is obvious that the effective SINR $_k$  is only affected by slowly-varying statistical CSI. Herein, perfect knowledge of the statistical CSI is assumed at the BS as in [12] and [15]. With the reduced computational complexity and feedback overhead under the two-timescale framework, the phase shift design of the active RIS is feasible with ease. Besides, the lower bound of the achievable sum rate is written as

$$R = \chi \sum_{k=1}^K \log_2(1 + \text{SINR}_k). \quad (30)$$

Next, we focus on analyzing the power scaling laws of the active RIS-aided system given the presence of a huge number of the BS antennas  $M$ , which is important for understanding the system's performance in large-scale configurations.

##### B. Power Scaling Laws

Within the massive MIMO system, transmit power is scaled down proportionally relative to the number of antennas in order to analyze the performance of the system [29]. Therefore, the power scaling laws of the active RIS-aided massive MIMO system considering RIS-aided channels with different Rician factors are discussed in this section. For the sake of clarity, we use  $a \geq 0$  to represent the factor that determines the level of power scaling, while  $E_u$  denotes a constant value during the power scaling.

*Corollary 3:* If the RIS-BS channel and the user-RIS channel are all Rician distributed, i.e.,  $\delta > 0$  and  $\varepsilon_k > 0, \forall k$ , we find that the achievable rate approaches zero as  $M \rightarrow \infty$  and the transmit power  $p$  of each user scales as  $p = E_u/M^a$ .

*Proof:* If  $p = E_u/M^a$  and  $M \rightarrow \infty$ , we retain the dominant part of  $E_k^{\text{signal}}(\Phi)$ ,  $E_k^{\text{leak}}(\Phi)$ ,  $I_{ki}(\Phi)$  and  $E_k^{\text{noise}}(\Phi)$ . Then the achievable rate can be written as (31) at the top of the next page, where

$$\text{DS}_k^{r,1} = \frac{|f_k(\Phi)|^4}{N^2} \Delta^2 c_k^2 \delta^2 \varepsilon_k^2 \rho^4, \quad (32)$$

$$\text{LE}_k^{r,1} = \frac{|f_k(\Phi)|^2}{N} \Delta^2 c_k^2 \delta^2 \varepsilon_k \rho^2 \{ \varepsilon_k (1 - \rho^2) + 1 \}, \quad (33)$$

$$\text{IN}_{i,k}^{r,1} = \frac{|f_k(\Phi)|^2}{N} \Delta^2 c_k \delta^2 \varepsilon_k c_i \rho^2 \left\{ \varepsilon_i \left( 1 - \rho^2 + \frac{\rho^2 |f_i(\Phi)|^2}{N} \right) + 1 \right\}, \quad (34)$$

$$\text{TN}_k^{r,1} = \frac{\beta}{N(\delta + 1)} \Delta^2 |f_k(\Phi)|^2 c_k \delta^2 \varepsilon_k \rho^2, \quad (35)$$

$$\text{SN}_k^{r,1} = \frac{|f_k(\Phi)|^2}{N} \Delta c_k \delta \varepsilon_k \rho^2. \quad (36)$$

With an asymptotic behavior of  $\mathcal{O}(M^{2-a})$ , the desired signal term,  $E_u M^{2-a} \text{DS}_k^{r,1}$ , has a lower order than the thermal

$$\text{SINR}_k = \frac{p |\mathbb{E} \{ \hat{\mathbf{q}}_k^H \mathbf{q}_k \}|^2}{p \left( \mathbb{E} \{ |\hat{\mathbf{q}}_k^H \mathbf{q}_k|^2 \} - |\mathbb{E} \{ \hat{\mathbf{q}}_k^H \mathbf{q}_k \}|^2 \right) + p \sum_{i=1, i \neq k}^K \mathbb{E} \{ |\hat{\mathbf{q}}_k^H \mathbf{q}_i|^2 \} + \eta^2 \sigma_e^2 \mathbb{E} \left\{ \left\| \hat{\mathbf{q}}_k^H \mathbf{H}_2 \Phi \Theta \right\|^2 \right\} + \sigma^2 \mathbb{E} \left\{ \left\| \hat{\mathbf{q}}_k \right\|^2 \right\}}. \quad (28)$$

$$\underline{R}_k^{(Ric,Ric)} = \chi \log_2 \left( 1 + \frac{E_u M^{2-a} \text{DS}_k^{r,1}}{E_u M^{2-a} \text{LE}_k^{r,1} + E_u M^{2-a} \sum_{i=1, i \neq k}^K \text{IN}_{i,k}^{r,1} + \sigma_e^2 M^2 \text{TN}_k^{r,1} + \sigma^2 M \text{SN}_k^{r,1}} \right), \quad (31)$$

$$\underline{R}_k^{(Ric,Ray)} = \chi \log_2 \left( 1 + \frac{E_u M^{2-a} \text{DS}_k^{r,2}}{E_u M^2 \text{LE}_k^{r,2} + E_u M^2 \sum_{i=1, i \neq k}^K \text{IN}_k^{r,2} + \sigma_e^2 M^{2+a} \text{TN}_k^{r,2} + \sigma^2 M \text{SN}_k^{r,2}} \right), \quad (37)$$

noise term,  $\sigma_e^2 M^2 \text{TN}_k^{r,1}$ , scaling as  $\mathcal{O}(M^2)$  in (31). Consequently, the achievable rate converges to zero. ■

This scenario exemplifies that the power scaling laws of  $M$  may not hold when the amplified thermal noise is present. Furthermore, we observe that the desired signal term is affected by the phase noise in the form of  $\rho^2$ , which is less than one according to Von Mises distribution. However, if there is no phase noise, i.e.,  $v$  approaches infinity, the desired signal power can be enhanced as  $\rho$  tends to one.

*Corollary 4:* If the user-RIS channel is Rayleigh distributed, i.e.,  $\varepsilon_k = 0, \forall k$ , and the RIS-BS channel is Rician distributed, i.e.,  $\delta > 0$ , the achievable rate of user  $k$  approaches zero, when  $p$  scales as  $p = E_u/M^a$  and  $M \rightarrow \infty$ .

*Proof :* By retaining the dominant part of each term in the SINR<sub>k</sub>, the achievable rate is given as (37) at the top of this page, where the specific expressions of the dominant part are given by

$$\text{DS}_k^{r,2} = \{ \Delta c_k (\delta e_{k2} + e_{k1}) + \gamma_k e_{k1} \}^2, \quad (38)$$

$$\text{LE}_k^{r,2} = \frac{\Delta^2 \sigma_e^2 \beta c_k}{\tau E_u (\delta + 1)} \left\{ \delta^2 e_{k2}^2 + \frac{1}{N} (2\delta e_{k1} e_{k2} + e_{k1}^2) \right\}, \quad (39)$$

$$\text{IN}_{i,k}^{r,2} = \frac{\Delta^2 \sigma_e^2 \beta c_i}{\tau E_u (\delta + 1)} \left\{ \delta^2 e_{k2}^2 + \frac{1}{N} (2\delta e_{k1} e_{k2} + e_{k1}^2) \right\}, \quad (40)$$

$$\text{TN}_k^{r,2} = \frac{\Delta^2 \delta \sigma_e^2 \beta^2 e_{k2}}{\tau E_u (\delta + 1)^2} \left( \delta e_{k2} + \frac{2e_{k1}}{N} \right), \quad (41)$$

$$\text{SN}_k^{r,2} = \Delta c_k \delta e_{k2} + \Delta c_k e_{k1} + \gamma_k e_{k1}, \quad (42)$$

where  $e_{k1}$  and  $e_{k2}$  scale as  $\mathcal{O}(M^{-a})$ . Hence, as a function of  $M$ , (38)-(41) behave asymptotically as  $\mathcal{O}(M^{-2a})$ , and (42) scales as  $\mathcal{O}(M^{-a})$ . As a result, the order of  $E_u M^{2-a} \text{DS}_k^{r,2}$  is  $\mathcal{O}(M^{2-3a})$  which is lower than that of the thermal noise term,  $\sigma_e^2 M^{2+a} \text{TN}_k^{r,2}$ , with an order of  $\mathcal{O}(M^{2-a})$ . Therefore, the achievable rate also tends to zero. ■

Likewise, the power scaling law “ $1/M^a$ ” is not applicable when the RIS-BS channel is Rician distributed.

*Corollary 5:* If the RIS-BS channel and the user-RIS channel are all Rayleigh distribution. With  $p = E_u/M^a$ , the achievable rate of user  $k$  approaches zero as  $M \rightarrow \infty$ .

*Proof :* When  $\delta = 0$ , we have  $a_{k1} = 0, a_{k2} = \Delta \beta \alpha_k + \gamma_k, a_{k3} = 0$  and  $e_{k3} = e_{k1}^2$ . By substituting these values into the expressions in Theorem 2, and ignoring the terms with lower order as  $M \rightarrow \infty$ , the achievable rate is written as (43) at the top of the next page, where the dominant terms are given as

$$\text{DS}_k^{r,3} = e_{k1}^2 (\Delta \beta \alpha_k + \gamma_k)^2, \quad (44)$$

$$\text{LE}_k^{r,3} = \frac{1}{N} e_{k1}^2 \Delta^2 \frac{\sigma_e^2}{\tau E_u} \beta^2 \alpha_k, \quad (45)$$

$$\text{IN}_{i,k}^{r,3} = \frac{1}{N} \Delta^2 e_{k1}^2 \beta^2 \alpha_i \frac{\sigma_e^2}{\tau E_u}, \quad (46)$$

$$\text{TN}_k^{r,3} = \underbrace{\frac{1}{N} e_{k1}^2 \Delta^2 \beta^2 \alpha_k}_{\text{TN}_{k,1}^{r,3}} + \underbrace{\Delta e_{k1}^2 \beta \frac{\Delta \sigma_e^2 \beta + \sigma^2}{\tau E_u}}_{\text{TN}_{k,2}^{r,3}}, \quad (47)$$

$$\text{SN}_k^{r,3} = e_{k1} (\Delta \beta \alpha_k + \gamma_k), \quad (48)$$

where  $e_{k1}$  scales as  $\mathcal{O}(M^{-a})$ . Therefore, (44)-(47) behave asymptotically as  $\mathcal{O}(M^{-2a})$ , and (48) scales as  $\mathcal{O}(M^{-a})$ .

However, the order of the thermal noise term depends on the factor  $a$ . If  $a \in (0, 1)$ , it scales with  $\mathcal{O}(M^{2-2a})$ . Otherwise, its asymptotic behavior is  $\mathcal{O}(M^{1-a})$ . Since the order of the desired signal term,  $E_u M^{2-a} \text{DS}_k^{r,3}$ , scaling as  $\mathcal{O}(M^{2-3a})$  is always lower than that of the thermal noise term,  $\sigma_e^2 M \left( M \text{TN}_{k,1}^{r,3} + M^a \text{TN}_{k,2}^{r,3} \right)$ , the achievable rate reaches zero. ■

Corollary 5 reveals that the power scaling law fails to hold for the considered system in the case where the channel between the RIS and the BS is Rayleigh distributed.

From Corollary 3 to Corollary 5, we draw some conclusions. Firstly, it is observed that the thermal noise introduced by the inherent structural characteristics [18] of the active RIS unavoidably appears in the dominant denominator for any given  $a$ . With an increase in  $M$ , the desired signal power gradually diminishes, whereas the power of the thermal noise amplified remains unaffected. Secondly, the phase noise exerts an impact on the SINR<sub>k</sub>, distinctly reflected in the desired signal power containing  $\rho^2$  in the scenario where all the channels are Rician distributed. While if  $\delta = 0$  or  $\varepsilon_k = 0$ , the impact disappears. Thirdly, as the achievable rate in (37) and (43) is independent of  $\Phi$ , any RIS phase shift yields the equivalent achievable rate when  $\delta = 0$  or  $\varepsilon_k = 0$ . Hence, designing the phase shifts is unnecessary if there are many scatterers between the BS and the RIS or between the users and the RIS.

Nevertheless, in large system parameter configuration, the power scaling laws become less critical. We can still leverage the active RIS to promote the system performance. This is because in practical deployment, the quantity of  $M$  is finite and what we need is simply to reduce the transmit power while still maintaining the communication.

$$\underline{R}_k^{(Ric,R)} = \chi \log_2 \left( 1 + \frac{E_u M^{2-a} DS_k^{r,3}}{E_u M^2 LE_k^{r,3} + E_u M^2 \sum_{i=1, i \neq k}^K IN_k^{r,3} + \sigma_e^2 M \left( MTN_{k,1}^{r,3} + M^a TN_{k,2}^{r,3} \right) + \sigma^2 MSN_k^{r,3}} \right), \quad (43)$$

Similar to the case of  $M$ , we can know the power scaling laws related to  $N$ , where the achievable rate is zero as  $N$  approaches infinity. The simulation results of power scaling laws with  $N$  will partly show in Section VI. In addition, increasing  $N$  can improve the active RIS-aided system's performance to a certain extent. However, considering the structure of active RISs, blindly increasing  $N$  will affect the allocation of power as more power being consumed to initiate RIS. On the other hand, high amplified power and transmit power can obviously help improve system performance. Therefore, it is necessary to consider the trade-off between the quantity of  $N$  and the power allocation, which needs further research work.

## V. DESIGN OF THE RIS PHASE SHIFTS

In this section, the optimization of phase shifts based on statistical CSI is considered. Specifically, as fairness among multiple users need to be ensured, this optimization aims to maximize minimum user achievable rate. Herein, we formulate the optimization problem as

$$\max_{\Phi} \min_{k \in \mathcal{K}} \underline{R}_k(\Phi), \quad (49)$$

$$\text{s.t. } 0 \leq \theta_n < 2\pi, \forall n, \quad (50)$$

where  $\underline{R}_k(\Phi)$  is given in Theorem 2,  $\Phi$  is the phase shift matrix, and  $\theta_n$  is the phase shift at the  $n$ -th element of the active RIS. Considering the complexity of  $\underline{R}_k(\Phi)$ , resolving the problem with conventional methods becomes challenging. By viewing the RIS phase shifts as the genes of a population, we apply the GA to tackle this optimization problem. Specifically, the fundamental concept of GA applied to RIS-aided systems involves treating the phase shift of each RIS element as the genetic code of a chromosome. Through iterative updates to these genetic codes, the population evolves. This eventually results in the RIS phase shifts being set to the most optimal codes identified in the last generation. Following that, we further discuss the specific procedural steps.

1) *Population initialization*: The initial population comprises  $N_p$  individuals. The chromosome of each individual is composed of  $N$  genes, where the  $n$ -th gene  $\theta_n$  is generated within  $[0, 2\pi)$ .

2) *Fitness evaluation and scaling*: In the current population, the fitness evaluation function for individual  $i$  with chromosome  $\Phi^i$  is defined as  $f_i = \min_k \underline{R}_k(\Phi^i)$ . Subsequently, the raw fitness scores derived from the fitness function undergo a scaling process to be adjusted within a range suitable for the selection function. Specifically, we sort the  $N_p$  individuals in descending order based on their raw fitness scores representing an individual's adaptation to the environment. An individual's position within the sorted scores corresponds to its rank, offering insight into its relative fitness level among the population. Individual  $i$  with rank  $r_i$  has scaled score proportional to  $\frac{1}{\sqrt{r_i}}$ ,

and the sum of the scaled values across the population equals the population size of parents for the next generation, which means that the expected fitness can be calculated as

$$f_i^e = \frac{1/\sqrt{r_i}}{\sum_{i=1}^{N_p} 1/\sqrt{r_i}}. \quad (51)$$

3) *Selection*: Then, we preserve  $N_e$  individuals with high expected fitness as elites for the next generation. Meanwhile, the stochastic universal sampling method given in Algorithm 1 is utilized twice to select  $2N_c$  parents for crossover. Specifically, we create a line where each parent is associated with a segment of the line, each segment's length is proportional to its expected fitness. The algorithm progresses along the line in uniform steps, assigning a parent from the segment it lands on at each step.

---

### Algorithm 1 Stochastic universal sampling

---

```

1: Input the step size  $p_{step} = 1/N_c$ , and set  $sum = 0$ ;
2: Randomly generate the initial pointer  $p_0 \in [0, p_{step}]$ ;
3: for  $j = 1 : N_c$  do
4:   for  $i = 1 : N_p$  do
5:      $sum = sum + f_i^e$ ;
6:     if  $p_0 < sum$  then
7:       Individual  $i$  becomes a parent and then break;
8:     end if
9:   end for
10:  Set  $sum = 0$ ,  $p_0 = p_0 + ip_{step}$ ;
11: end for

```

---

4) *Crossover*: After selecting parents, we combine two individuals to produce a crossover offspring for the subsequent generation. The procedure for crossover is outlined in Algorithm 2.

---

### Algorithm 2 Single-point Crossover

---

```

1: Input the selected parents
2: for  $i = 1 : N_c$  do
3:   Select the  $(2i - 1)$ -th and  $2i$ -th as the parents;
4:   Generate a random integer  $n$ ,  $n \in [1, N]$ ;
5:   Choose vector entries with numbers  $\leq n$  from the first parent. Select vector entries with numbers  $> n$  from the other parent. The child has a chromosome
    $\text{diag} \left\{ e^{j\theta_1^{2i-1}}, \dots, e^{j\theta_n^{2i-1}}, e^{j\theta_{n+1}^{2i}}, \dots, e^{j\theta_N^{2i}} \right\}$ ;
6: end for

```

---

5) *Mutation*: Afterwards,  $N_m$  mutated offspring are generated as in Algorithm 3, where the  $i$ -th offspring is reproduced by mutating each gene of  $i$ -th parent under a probability  $p_m$ .

---

**Algorithm 3** Mutation
 

---

```

1: for  $i = 1 : N_m$  do
2:   for  $n = 1 : N$  do
3:     Generate  $c$  randomly from  $(0,1)$ ;
4:     if  $c < p_m$  then
5:       The  $n$ -th entry  $e^{j\theta_n^i}$  in chromosome of parent  $i$ 
         mutates to a value randomly selected from a
         uniform distribution in  $[0, 2\pi)$ ;
6:     end if
7:   end for
8: end for
  
```

---

After performing these procedures, we obtain the next generation composed of  $N_e$  elites,  $N_c$  offspring generated through crossover and  $N_m$  offspring produced by mutation. The algorithm will stop when it reaches the maximum number of iterations  $100N$  or the average change of the raw fitness is lower than  $10^{-4}$ . As a result, the GA algorithm outputs the chromosome of the individual with the highest fitness in the current population.

## VI. NUMERICAL RESULTS

In this section, we present numerical simulations that are conducted to evaluate the influence of important parameters on the performance of an active RIS-aided massive MIMO system. With a setup similar to [16], we posit an assumption where  $K = 8$  users are evenly distributed along a semicircle with the active RIS as the center and a radius  $r_{UR}$  of 20 m. The distance from the RIS to the BS is  $d_{RB} = 700$  m. While the distance between user  $k$  and the BS is calculated as  $d_k^{UB} = \sqrt{(d_{RB} - r_{UR}\cos(\frac{\pi}{9}k))^2 + (r_{UR}\sin(\frac{\pi}{9}k))^2}$ . Owing to the long distance between users and the BS, coupled with the presence of obstacles, the direct links suffer severe attenuation compared to the RIS-aided links, i.e., the path-loss exponent of the direct links exceeds that of the RIS-aided links. Therefore, the large-scale fading coefficients for user-RIS channel, RIS-BS channel and user-BS channel are modeled respectively as  $\alpha_k = 10^{-3}r_{UR}^{-2}$ ,  $\beta = 10^{-3}d_{RB}^{-2.8}$  and  $\gamma_k = 10^{-3}d_k^{UB-4.2}, \forall k$ . Each coherence block, as our assumption, comprises  $\tau_c = 196$  symbols, out of which  $\tau = 8$  symbols are utilized for channel estimation. Furthermore, we set the static noise power as  $\sigma^2 = -104$  dBm and the thermal noise power as  $\sigma_e^2 = -70$  dBm. Moreover, we consider systems with passive RIS and those without RIS in the absence of phase noise for comparison. Meanwhile, for the phase noise at the active RIS, we have the concentration parameter  $v = 2$ .

Differing from passive RIS that has zero direct-current (DC) power consumption, active RIS reflecting elements need the suitable DC biasing power to operate [30]. As a result, the total power consumption of the uplink active RIS-aided system is given by

$$P_{total} = \sum_{k=1}^K p + P_{cir} + \xi^{-1}P_A, \quad (52)$$

where  $P_{cir} = N(P_{SC} + P_{DC})$  is the circuit power. Specifically, the power consumption of the switch and control (SC) circuit at each reflecting element is denoted by  $P_{SC}$  and the power consumption of DC is expressed as  $P_{DC}$ . Besides,  $\xi$

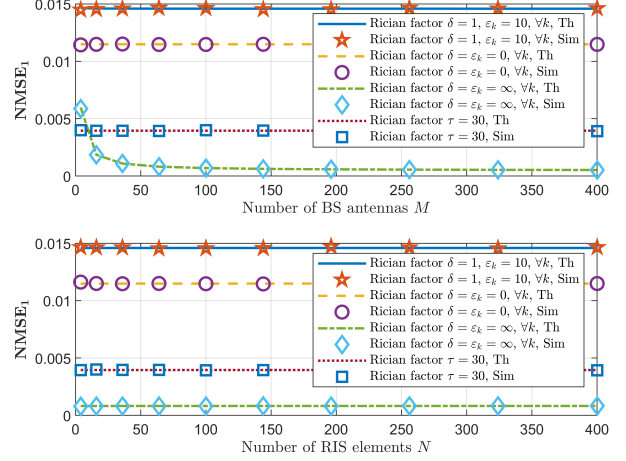


Fig. 2. NMSE of user 1 versus the number of antennas  $M$  and the number of RIS elements  $N$ .

$= 0.8$  is the amplifier efficiency. It is noted that if  $P_{total} \leq N(P_{SC} + P_{DC})$ , the active RIS does not work, and a similar situation applies to passive RIS when  $P_p \leq NP_{SC}$  where  $P_p$  is the total power consumption in the passive RIS-aided system. Herein, we take into account that the  $P_{SC} = -10$  dBm and  $P_{DC} = -5$  dBm. Unless explicitly stated otherwise, we assume  $P_{total} = 20$  dBm for all systems. Furthermore, an equal power splitting scheme is adopted, where  $\xi^{-1}P_A = \sum_{k=1}^K p$ . Additionally, the lines labeled as ‘‘Simulation’’ follow from (28), whereas those marked as ‘‘Theory’’ are acquired based on (29).

To begin with, we evaluate the NMSE and neglect the power consumption of RIS circuits for the simplicity of analysis. In Fig. 2, we illustrate the NMSE of user 1 against the number of  $M$  and  $N$ . Generally speaking, the NMSE is not particularly sensitive to changes in  $M$  and  $N$ , except that it is a decreasing function as  $M$  increases when  $\delta = \epsilon_k \rightarrow \infty$ . Also, through the extension of the pilot signals to 30, a decrease in NMSE is noted. Furthermore, we observe that, unlike passive RIS, the NMSE of active RIS-aided system is not dependent on  $N$ . This implies that there is no need to sacrifice deployment costs for smaller NMSE. This further corroborates the findings in Corollary 1.

In Fig. 3, we present the relationship between the total power and achievable sum rate. Initially, the achievable sum rate of the passive RIS-aided system slightly exceeds that of the active counterpart primarily. This is because of the active RIS’s additional power requirements for startup, reducing the available power for amplification and transmission. However, as the total power increases, the achievable rate of the active RIS-aided system surpasses that of the passive counterpart. Furthermore, the GA algorithm we discuss in Section V contributes to achieving better performance when applied to the phase shifts of both active and passive RIS, compared to random fixed phase shifts.

Fig. 4 illustrates how the achievable sum rate exhibits variations corresponding to the number of BS antennas  $M$



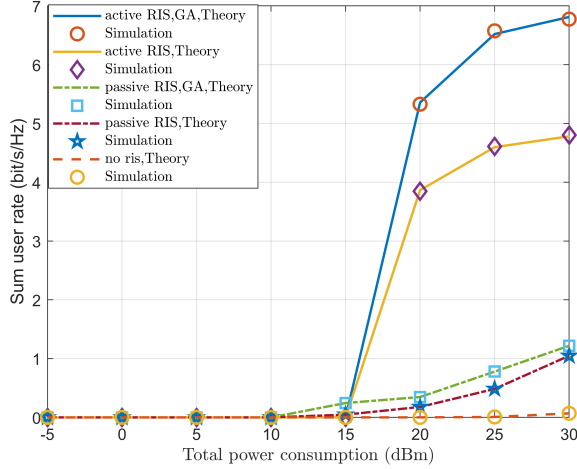


Fig. 3. Uplink achievable sum rate versus total power consumption.

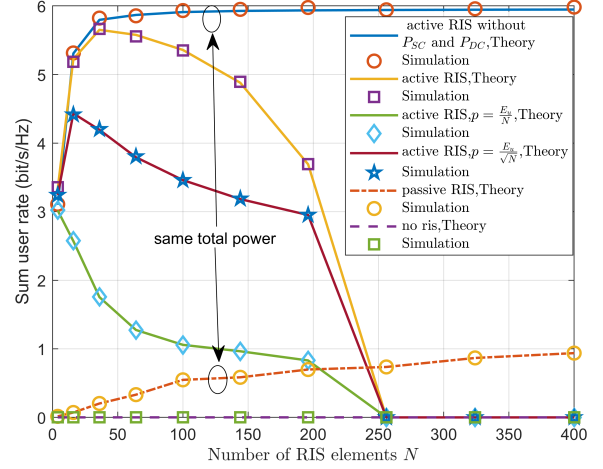


Fig. 5. Uplink achievable sum rate versus the number of RIS elements  $N$ .

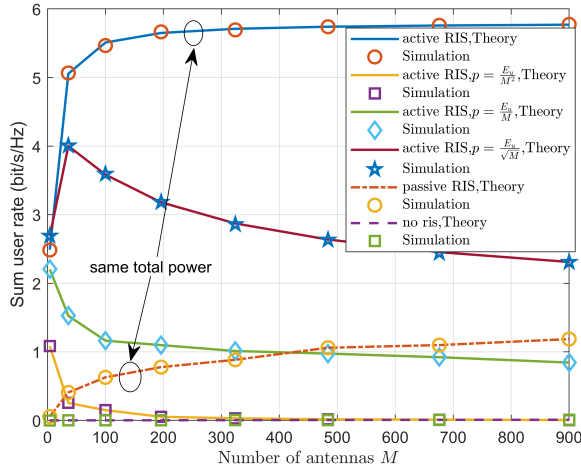


Fig. 4. Uplink achievable sum rate versus the number of antennas  $M$ .

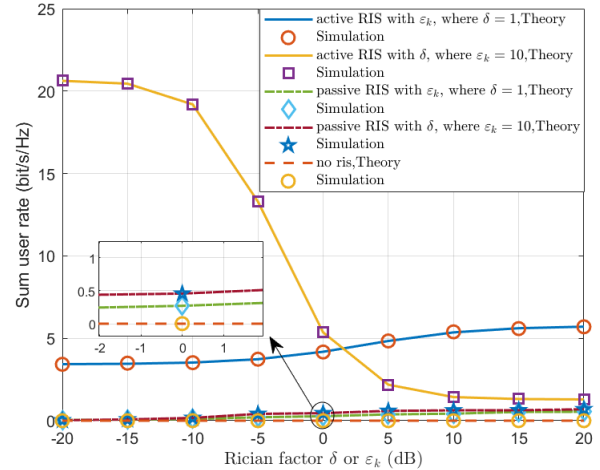


Fig. 6. Uplink achievable sum rate versus rician factor  $\delta$  or  $\epsilon_k$ .

when utilizing the optimized phase shifts. Remarkably, as  $M$  grows, the sum rate of active RIS-aided system exhibits an increase and its trend behaves similarly to that of passive RIS-aided system. Despite the rate approaching saturation as  $M$  increases, the active RIS-aided system consistently maintains a significantly higher rate compared to the passive counterpart. Then we use the example of Rician channels to illustrate intuitively why the power scaling laws are not applicable to active RIS-aided system. Specifically, the transmit power is scaled down by  $p = \frac{E_u}{M}$ ,  $p = \frac{E_u}{\sqrt{M}}$  and  $p = \frac{E_u}{M^2}$  with  $E_u = 10$  dBm respectively. From Fig. 4, we observe that as  $M$  increases, the rate shows a progressive decrease instead of remaining constant, due to the rapid power scaling down. If we further increase  $M$ , the rate is expected to eventually converge to zero.

Fig. 5 shows the achievable sum rate with respect to the number of elements  $N$  with optimized phase shifts. Similarly, the achievable sum rate of the active RIS-aided system markedly surpasses than that of the passive counterpart. If we neglect the power consumption of active RIS circuits, the rate

experiences an increase as  $N$  grows, but it quickly reaches saturation. If we scale down the transmit power proportionally to  $\frac{1}{N}$  and  $\frac{1}{\sqrt{N}}$ , we still find that the power scaling laws are not applicable to active RIS-aided system, in fact, worsens the situation. In particular, the reduction in the sum rate occurs initially because the transmit power is scaled down, while the thermal noise remains unaffected. This results in the desired power being relatively small compared to the thermal noise. When  $N$  increases, the RIS requires huge power support as the circuit power consumption has a linear relationship with  $N$ , which results in the majority of power being allocated to the circuits in active RIS elements. Therefore, in large scale configuration of  $N$ , the achievable rate immediately approaches zero due to insufficient power for the circuits in the RIS elements. Hence, in practice, the number of  $N$  should be smaller to better leverage the role of active RIS within the system.

In Fig. 6, the achievable sum rate experiences a decline as  $\delta$  increases, while it demonstrates an upward trend with the rise of  $\epsilon_k$  in the active RIS-aided system. This is because

when  $\delta$  is small, the RIS-BS channel is rich scattering, which increases the spatial multiplexing gains, thereby improving the performance of the system. While with increasing  $\delta$ , the rank of the RIS-BS channel converges to one, which is not conducive to spatial multiplexing for multiple users, leading to a low achievable rate [31]. On the other hand, as  $\varepsilon_k$  increases, the user-RIS channels become LoS-dominant, providing better beamforming gain [32]. Also, it's interesting to find that in the case of relatively low total power, increasing  $\delta$  can actually improve the achievable sum rate in the passive RIS-aided system.

## VII. CONCLUSION

In this work, we delved into the closed-form expressions of an active RIS-aided massive MIMO system, taking into account the influence of the phase noise, within the framework of a two-timescale design scheme. Specifically, we considered Rician fading for RIS-aided channels and Rayleigh fading for the direct links. Then we utilized the LMMSE channel estimator for the aggregated channels with the MRC detector to receive signals. The UatF bound of achievable rate was derived in the closed-form, depending only on statistical CSI. Subsequently, we investigated the power scaling laws, revealing that scaling the transmit power by  $1/M^a$  or  $1/N^a$  does not allow for maintaining a non-zero achievable rate in the active RIS-aided system. Furthermore, we performed a GA-based method to optimize the phase shifts of the active RIS. Our results validated the consistently superior performance of an active RIS-aided system even when subjected to phase noise, compared to the passive counterpart under different system parameters.

## APPENDIX A

### PROOF OF SOME USEFUL RESULTS

First, we review some useful lemmas used in the following computations.

*Lemma 3:* Considering the deterministic matrix  $\bar{\mathbf{h}}_k \bar{\mathbf{h}}_k^H \in \mathbb{C}^{N \times N}$  and the random phase noise matrix  $\Theta \in \mathbb{C}^{N \times N}$ , we have

$$\mathbb{E} \left\{ \Theta \bar{\mathbf{h}}_k \bar{\mathbf{h}}_k^H \Theta^H \right\} = \rho^2 \bar{\mathbf{h}}_k \bar{\mathbf{h}}_k^H + (1 - \rho^2) \mathbf{I}_N. \quad (53)$$

*Proof:* We define  $[\mathbf{X}]_{mn}$  as the entry in the  $m$ -th row and  $n$ -th column of matrix  $\mathbf{X}$ . Since the PDF of  $\theta_n$  is symmetric, there's  $\mathbb{E} \left\{ e^{j\theta_m} \right\} = \mathbb{E} \left\{ e^{-j\theta_n} \right\} = \rho$ . When  $m \neq n$ , we can get

$$\begin{aligned} \left[ \mathbb{E} \left\{ \Theta \bar{\mathbf{h}}_k \bar{\mathbf{h}}_k^H \Theta^H \right\} \right]_{mn} &= \left[ \bar{\mathbf{h}}_k \bar{\mathbf{h}}_k^H \right]_{mn} \mathbb{E} \left\{ e^{j\theta_m - j\theta_n} \right\} \\ &= \rho^2 \left[ \bar{\mathbf{h}}_k \bar{\mathbf{h}}_k^H \right]_{mn}. \end{aligned} \quad (54)$$

With  $\text{diag} \left\{ \bar{\mathbf{h}}_k \bar{\mathbf{h}}_k^H \right\} = \mathbf{I}_N$ , we obtain that

$$\begin{aligned} \mathbb{E} \left\{ \Theta \bar{\mathbf{h}}_k \bar{\mathbf{h}}_k^H \Theta^H \right\} &= \rho^2 \bar{\mathbf{h}}_k \bar{\mathbf{h}}_k^H + (1 - \rho^2) \text{diag} \left\{ \bar{\mathbf{h}}_k \bar{\mathbf{h}}_k^H \right\} \\ &= \rho^2 \bar{\mathbf{h}}_k \bar{\mathbf{h}}_k^H + (1 - \rho^2) \mathbf{I}_N. \end{aligned} \quad (55)$$

Then, we complete the proof.  $\blacksquare$

*Lemma 4:* As in [16], we take into account a matrix  $\mathbf{X} \in \mathbb{C}^{M \times N}$ , whose entries are i.i.d. with zero mean and  $v_x$  variance. With a deterministic matrix  $\mathbf{D} \in \mathbb{C}^{N \times N}$ , we have

$$\mathbb{E} \left\{ \mathbf{X} \mathbf{D} \mathbf{X}^H \right\} = v_x \text{Tr} \left\{ \mathbf{D} \right\} \mathbf{I}_M. \quad (56)$$

For both deterministic matrices  $\mathbf{C} \in \mathbb{C}^{M \times M}$  and  $\mathbf{D} \in \mathbb{C}^{N \times N}$ , if  $\mathbf{C} = \mathbf{C}^H$ , we have

$$\begin{aligned} &\mathbb{E} \left\{ \tilde{\mathbf{H}}_2^H \mathbf{C} \tilde{\mathbf{H}}_2 \mathbf{D} \tilde{\mathbf{H}}_2^H \mathbf{C} \tilde{\mathbf{H}}_2 \right\} \\ &= \text{Tr} \left\{ \mathbf{D} \right\} \text{Tr} \left\{ \mathbf{C}^2 \right\} \mathbf{I}_N + |\text{Tr} \left\{ \mathbf{C} \right\}|^2 \mathbf{D}. \end{aligned} \quad (57)$$

## APPENDIX B PROOF OF LEMMA 1

Referring to  $\mathbf{y}_p^k$  where  $\tilde{\mathbf{H}}_2$ ,  $\tilde{\mathbf{h}}_k$ ,  $\tilde{\mathbf{d}}_k$ ,  $\mathbf{V}$  and  $\mathbf{N}$  are mutually independent with zero-mean and  $\mathbb{E} \left\{ e^{j\theta_m} \right\} = \rho$ , we have

$$\begin{aligned} \mathbb{E} \left\{ \mathbf{y}_p^k \right\} &= \mathbb{E} \left\{ \mathbf{q}_k \right\} + \frac{\eta}{\sqrt{\tau p}} \mathbb{E} \left\{ \mathbf{H}_2 \Phi \Theta \mathbf{V} \mathbf{s}_k \right\} + \frac{1}{\sqrt{\tau p}} \mathbb{E} \left\{ \mathbf{N} \mathbf{s}_k \right\} \\ &= \eta \rho \sqrt{c_k \delta \varepsilon_k} \bar{\mathbf{H}}_2 \Phi \bar{\mathbf{h}}_k. \end{aligned} \quad (58)$$

As a result, the covariance matrix between the channel  $\mathbf{q}_k$  and the observation vector  $\mathbf{y}_p^k$  can be expressed respectively as

$$\begin{aligned} \text{Cov} \left\{ \mathbf{q}_k, \mathbf{y}_p^k \right\} &= \mathbb{E} \left\{ (\mathbf{q}_k - \mathbb{E} \left\{ \mathbf{q}_k \right\}) (\mathbf{y}_p^k - \mathbb{E} \left\{ \mathbf{y}_p^k \right\})^H \right\} \\ &= \mathbb{E} \left\{ (\mathbf{q}_k - \mathbb{E} \left\{ \mathbf{q}_k \right\}) \right. \\ &\quad \left. \times \left( \mathbf{q}_k + \frac{\eta}{\sqrt{\tau p}} \mathbf{H}_2 \Phi \Theta \mathbf{V} \mathbf{s}_k + \frac{1}{\sqrt{\tau p}} \mathbf{N} \mathbf{s}_k - \mathbb{E} \left\{ \mathbf{q}_k \right\} \right)^H \right\} \\ &= \mathbb{E} \left\{ (\mathbf{q}_k - \mathbb{E} \left\{ \mathbf{q}_k \right\}) (\mathbf{q}_k - \mathbb{E} \left\{ \mathbf{q}_k \right\})^H \right\} \\ &= \text{Cov} \left\{ \mathbf{q}_k, \mathbf{q}_k \right\}. \end{aligned} \quad (59)$$

and we have

$$\begin{aligned} \text{Cov} \left\{ \mathbf{y}_p^k, \mathbf{q}_k \right\} &= (\text{Cov} \left\{ \mathbf{q}_k, \mathbf{y}_p^k \right\})^H \\ &= (\text{Cov} \left\{ \mathbf{q}_k, \mathbf{q}_k \right\})^H = \text{Cov} \left\{ \mathbf{q}_k, \mathbf{q}_k \right\}. \end{aligned} \quad (60)$$

With the definition of  $\mathbf{q}_k$ ,  $\text{Cov} \left\{ \mathbf{q}_k, \mathbf{q}_k \right\}$  can be written as  $\text{Cov} \left\{ \mathbf{q}_k, \mathbf{q}_k \right\}$

$$\begin{aligned} &= \mathbb{E} \left\{ \left( \eta \sqrt{c_k \delta \varepsilon_k} \bar{\mathbf{H}}_2 \Phi \Theta \bar{\mathbf{h}}_k + \eta \sqrt{c_k \delta} \bar{\mathbf{H}}_2 \Phi \Theta \tilde{\mathbf{h}}_k \right. \right. \\ &\quad \left. \left. + \eta \sqrt{c_k \varepsilon_k} \tilde{\mathbf{H}}_2 \Phi \Theta \bar{\mathbf{h}}_k + \eta \sqrt{c_k} \tilde{\mathbf{H}}_2 \Phi \Theta \tilde{\mathbf{h}}_k + \sqrt{\gamma_k} \tilde{\mathbf{d}}_k \right. \right. \\ &\quad \left. \left. - \eta \rho \sqrt{c_k \delta \varepsilon_k} \bar{\mathbf{H}}_2 \Phi \bar{\mathbf{h}}_k \right) \times \left( \mathbf{q}_k - \eta \rho \sqrt{c_k \delta \varepsilon_k} \bar{\mathbf{H}}_2 \Phi \bar{\mathbf{h}}_k \right)^H \right\}. \end{aligned} \quad (61)$$

Then, the first term in  $\text{Cov} \left\{ \mathbf{q}_k, \mathbf{q}_k \right\}$  can be calculated as

$$\begin{aligned} &\mathbb{E} \left\{ \left( \eta \sqrt{c_k \delta \varepsilon_k} \bar{\mathbf{H}}_2 \Phi \Theta \bar{\mathbf{h}}_k \right) \left( \mathbf{q}_k - \eta \rho \sqrt{c_k \delta \varepsilon_k} \bar{\mathbf{H}}_2 \Phi \bar{\mathbf{h}}_k \right)^H \right\} \\ &= \mathbb{E} \left\{ \left( \eta \sqrt{c_k \delta \varepsilon_k} \bar{\mathbf{H}}_2 \Phi \Theta \bar{\mathbf{h}}_k \right) \right. \\ &\quad \left. \times \left( \eta \sqrt{c_k \delta \varepsilon_k} \bar{\mathbf{h}}_k^H \Theta^H \Phi^H \bar{\mathbf{H}}_2^H - \eta \rho \sqrt{c_k \delta \varepsilon_k} \bar{\mathbf{H}}_2 \Phi \bar{\mathbf{h}}_k \right)^H \right\} \\ &= \eta^2 c_k \delta \varepsilon_k \bar{\mathbf{H}}_2 \Phi \mathbb{E} \left\{ \Theta \bar{\mathbf{h}}_k \bar{\mathbf{h}}_k^H \Theta^H \right\} \Phi^H \bar{\mathbf{H}}_2^H \\ &\quad - \eta^2 \rho c_k \delta \varepsilon_k \bar{\mathbf{H}}_2 \Phi \mathbb{E} \left\{ \Theta \right\} \bar{\mathbf{h}}_k \bar{\mathbf{h}}_k^H \Phi^H \bar{\mathbf{H}}_2^H \\ &= \eta^2 (1 - \rho^2) c_k \delta \varepsilon_k N \mathbf{a}_M \mathbf{a}_M^H. \end{aligned} \quad (62)$$

The remaining terms are obtained by using a similar procedure. Therefore we have

APPENDIX C  
PROOF OF THEOREM 1

$$\begin{aligned} & \mathbb{E} \left\{ \left( \eta \sqrt{c_k \delta \bar{\mathbf{H}}_2 \Phi \Theta \tilde{\mathbf{h}}_k} \right) \left( \mathbf{q}_k - \eta \rho \sqrt{c_k \delta \varepsilon_k \bar{\mathbf{H}}_2 \Phi \bar{\mathbf{h}}_k} \right)^H \right\} \\ &= \mathbb{E} \left\{ \left( \eta \sqrt{c_k \delta \bar{\mathbf{H}}_2 \Phi \Theta \tilde{\mathbf{h}}_k} \right) \left( \eta \sqrt{c_k \delta \bar{\mathbf{H}}_2 \Phi \Theta \tilde{\mathbf{h}}_k} \right)^H \right\} \\ &= \eta^2 c_k \delta N \mathbf{a}_M \mathbf{a}_M^H, \end{aligned} \quad (63)$$

$$\begin{aligned} & \mathbb{E} \left\{ \left( \eta \sqrt{c_k \varepsilon_k \tilde{\mathbf{H}}_2 \Phi \Theta \bar{\mathbf{h}}_k} \right) \left( \mathbf{q}_k - \eta \rho \sqrt{c_k \delta \varepsilon_k \bar{\mathbf{H}}_2 \Phi \bar{\mathbf{h}}_k} \right)^H \right\} \\ &= \mathbb{E} \left\{ \left( \eta \sqrt{c_k \varepsilon_k \tilde{\mathbf{H}}_2 \Phi \Theta \bar{\mathbf{h}}_k} \right) \left( \eta \sqrt{c_k \varepsilon_k \tilde{\mathbf{H}}_2 \Phi \Theta \bar{\mathbf{h}}_k} \right)^H \right\} \\ &= \eta^2 c_k \varepsilon_k N \mathbf{I}_M, \end{aligned} \quad (64)$$

$$\begin{aligned} & \mathbb{E} \left\{ \eta \sqrt{c_k \tilde{\mathbf{H}}_2 \Phi \Theta \tilde{\mathbf{h}}_k} \left( \mathbf{q}_k - \eta \rho \sqrt{c_k \delta \varepsilon_k \bar{\mathbf{H}}_2 \Phi \bar{\mathbf{h}}_k} \right)^H \right\} \\ &= \mathbb{E} \left\{ \eta \sqrt{c_k \tilde{\mathbf{H}}_2 \Phi \Theta \tilde{\mathbf{h}}_k} \left( \eta \sqrt{c_k \tilde{\mathbf{H}}_2 \Phi \Theta \tilde{\mathbf{h}}_k} \right)^H \right\} \\ &= \eta^2 c_k N \mathbf{I}_M, \end{aligned} \quad (65)$$

$$\begin{aligned} & \mathbb{E} \left\{ \sqrt{\gamma_k} \tilde{\mathbf{d}}_k \left( \mathbf{q}_k - \eta \rho \sqrt{c_k \delta \varepsilon_k \bar{\mathbf{H}}_2 \Phi \bar{\mathbf{h}}_k} \right)^H \right\} \\ &= \mathbb{E} \left\{ \sqrt{\gamma_k} \tilde{\mathbf{d}}_k \sqrt{\gamma_k} \tilde{\mathbf{d}}_k^H \right\} = \gamma_k \mathbf{I}_M, \end{aligned} \quad (66)$$

$$\begin{aligned} & \mathbb{E} \left\{ \left( -\eta \rho \sqrt{c_k \delta \varepsilon_k \bar{\mathbf{H}}_2 \Phi \bar{\mathbf{h}}_k} \right) \left( \mathbf{q}_k - \eta \rho \sqrt{c_k \delta \varepsilon_k \bar{\mathbf{H}}_2 \Phi \bar{\mathbf{h}}_k} \right)^H \right\} \\ &= \mathbb{E} \left\{ \left( -\eta \rho \sqrt{c_k \delta \varepsilon_k \bar{\mathbf{H}}_2 \Phi \bar{\mathbf{h}}_k} \right) \left( \eta \sqrt{c_k \delta \varepsilon_k \bar{\mathbf{H}}_2 \Phi \Theta \bar{\mathbf{h}}_k} \right)^H \right. \\ & \quad \left. + \left( -\eta \rho \sqrt{c_k \delta \varepsilon_k \bar{\mathbf{H}}_2 \Phi \bar{\mathbf{h}}_k} \right) \left( -\eta \sqrt{c_k \delta \varepsilon_k \bar{\mathbf{H}}_2 \Phi \Theta \bar{\mathbf{h}}_k} \right)^H \right\} \\ &= 0. \end{aligned} \quad (67)$$

Thus, the covariance matrix can be obtained as

$$\begin{aligned} & \text{Cov}\{\mathbf{q}_k, \mathbf{q}_k\} \\ &= \eta^2 (1 - \rho^2) c_k \delta \varepsilon_k N \mathbf{a}_M \mathbf{a}_M^H + \eta^2 c_k \delta N \mathbf{a}_M \mathbf{a}_M^H \\ & \quad + \eta^2 c_k \varepsilon_k N \mathbf{I}_M + \eta^2 c_k N \mathbf{I}_M + \gamma_k \mathbf{I}_M + 0 \\ & \triangleq a_{k1} \mathbf{a}_M \mathbf{a}_M^H + a_{k2} \mathbf{I}_M, \end{aligned} \quad (68)$$

where we define  $a_{k1} = \Delta c_k \delta \{ \varepsilon_k (1 - \rho^2) + 1 \}$ , and  $a_{k2} = \Delta c_k (\varepsilon_k + 1) + \gamma_k$ .

Therefore,  $\text{Cov}\{\mathbf{y}_p^k, \mathbf{y}_p^k\}$  can be expressed as

$$\begin{aligned} & \text{Cov}\{\mathbf{y}_p^k, \mathbf{y}_p^k\} = \mathbb{E} \left\{ (\mathbf{y}_p^k - \mathbb{E}\{\mathbf{y}_p^k\}) (\mathbf{y}_p^k - \mathbb{E}\{\mathbf{y}_p^k\})^H \right\} \\ &= \mathbb{E} \left\{ (\mathbf{q}_k - \mathbb{E}\{\mathbf{q}_k\}) (\mathbf{q}_k - \mathbb{E}\{\mathbf{q}_k\})^H \right\} + \frac{1}{\tau p} \mathbb{E} \left\{ \mathbf{N} \mathbf{s}_k \mathbf{s}_k^H \mathbf{N}^H \right\} \\ & \quad + \mathbb{E} \left\{ \left( \frac{\eta}{\sqrt{\tau p}} \mathbf{H}_2 \Phi \Theta \mathbf{V} \mathbf{s}_k \right) \left( \frac{\eta}{\sqrt{\tau p}} \mathbf{H}_2 \Phi \Theta \mathbf{V} \mathbf{s}_k \right)^H \right\} \\ &= \text{Cov}\{\mathbf{q}_k, \mathbf{q}_k\} + \frac{\sigma^2}{\tau p} \mathbf{I}_M + \frac{\eta^2 \sigma_e^2 \beta}{\tau p (\delta + 1)} \mathbb{E} \left\{ \delta \bar{\mathbf{H}}_2 \bar{\mathbf{H}}_2^H + \tilde{\mathbf{H}}_2 \tilde{\mathbf{H}}_2^H \right\} \\ &= \text{Cov}\{\mathbf{q}_k, \mathbf{q}_k\} + \frac{\sigma^2}{\tau p} \mathbf{I}_M + \frac{\eta^2 \sigma_e^2 \beta N \delta}{\tau p (\delta + 1)} \mathbf{a}_M \mathbf{a}_M^H + \frac{\eta^2 \sigma_e^2 \beta N}{\tau p (\delta + 1)} \mathbf{I}_M \\ &= (a_{k1} + \varpi \delta) \mathbf{a}_M \mathbf{a}_M^H + \left( a_{k2} + \frac{\sigma^2}{\tau p} + \varpi \right) \mathbf{I}_M^H \\ & \triangleq m_k \mathbf{a}_M \mathbf{a}_M^H + n_k \mathbf{I}_M, \end{aligned} \quad (69)$$

where  $m_k = a_{k1} + \varpi \delta$  and  $n_k = a_{k2} + \frac{\sigma^2}{\tau p} + \varpi$ .

Based on the observation vector  $\mathbf{y}_p^k$ , the LMMSE estimate of the channel  $\mathbf{q}_k$  is formulated as in [33], and we have

$$\hat{\mathbf{q}}_k = \mathbb{E}\{\mathbf{q}_k\} + \text{Cov}\{\mathbf{q}_k, \mathbf{y}_p^k\} \text{Cov}^{-1}\{\mathbf{y}_p^k, \mathbf{y}_p^k\} (\mathbf{y}_p^k - \mathbb{E}\{\mathbf{y}_p^k\}). \quad (70)$$

For the  $\text{Cov}^{-1}\{\mathbf{y}_p^k, \mathbf{y}_p^k\}$  as in [33], we can get

$$\text{Cov}^{-1}\{\mathbf{y}_p^k, \mathbf{y}_p^k\} = n_k^{-1} \mathbf{I}_M - \frac{m_k (n_k)^{-2}}{1 + M m_k n_k^{-1}} \mathbf{a}_M \mathbf{a}_M^H, \quad (71)$$

where  $m_k$  and  $n_k$  are defined in (69). As a result, we obtain that

$$\begin{aligned} & \text{Cov}\{\mathbf{q}_k, \mathbf{y}_p^k\} \text{Cov}^{-1}\{\mathbf{y}_p^k, \mathbf{y}_p^k\} \\ &= (a_{k1} \mathbf{a}_M \mathbf{a}_M^H + a_{k2} \mathbf{I}_M) \left\{ n_k^{-1} \mathbf{I}_M - \frac{m_k (n_k)^{-2}}{1 + M m_k n_k^{-1}} \mathbf{a}_M \mathbf{a}_M^H \right\} \\ &= \frac{\left\{ \left( \frac{\sigma^2}{\tau p} + \varpi \right) a_{k1} - \varpi \delta a_{k2} \right\} \mathbf{a}_M \mathbf{a}_M^H}{(a_{k2} + \frac{\sigma^2}{\tau p} + \varpi)^2 + M (a_{k1} + \varpi \delta) (a_{k2} + \frac{\sigma^2}{\tau p} + \varpi)} + \frac{a_{k2}}{n_k} \mathbf{I}_M \\ & \triangleq a_{k3} \mathbf{a}_M \mathbf{a}_M^H + a_{k4} \mathbf{I}_M \triangleq \mathbf{A}_k = \mathbf{A}_k^H. \end{aligned} \quad (72)$$

Thus, the LMMSE channel estimate of  $\mathbf{q}_k$  is calculated as

$$\begin{aligned} \hat{\mathbf{q}}_k &= \mathbb{E}\{\mathbf{q}_k\} + \text{Cov}\{\mathbf{q}_k, \mathbf{y}_p^k\} \text{Cov}^{-1}\{\mathbf{y}_p^k, \mathbf{y}_p^k\} (\mathbf{y}_p^k - \mathbb{E}\{\mathbf{y}_p^k\}) \\ &= \eta \rho \sqrt{c_k \delta \varepsilon_k \bar{\mathbf{H}}_2 \Phi \bar{\mathbf{h}}_k} + \mathbf{A}_k (\mathbf{y}_p^k - \mathbb{E}\{\mathbf{y}_p^k\}) \\ &= \mathbf{A}_k \mathbf{y}_p^k + (\mathbf{I}_M - \mathbf{A}_k) \eta \rho \sqrt{c_k \delta \varepsilon_k \bar{\mathbf{H}}_2 \Phi \bar{\mathbf{h}}_k} \\ & \triangleq \mathbf{A}_k \mathbf{y}_p^k + \mathbf{B}_k, \end{aligned} \quad (73)$$

where  $\mathbf{B}_k = (\mathbf{I}_M - \mathbf{A}_k) \eta \rho \sqrt{c_k \delta \varepsilon_k \bar{\mathbf{H}}_2 \Phi \bar{\mathbf{h}}_k}$ .

Then we rewrite the above expression as

$$\begin{aligned} \hat{\mathbf{q}}_k &= \mathbf{A}_k \left( \mathbf{q}_k + \frac{\eta}{\sqrt{\tau p}} \mathbf{H}_2 \Phi \Theta \mathbf{V} \mathbf{s}_k + \frac{1}{\sqrt{\tau p}} \mathbf{N} \mathbf{s}_k \right) + \mathbf{B}_k \\ &= \mathbf{A}_k \left( \sum_{w=1}^4 \mathbf{q}_k^w + \mathbf{d}_k \right) + \mathbf{A}_k \frac{\eta}{\sqrt{\tau p}} \mathbf{H}_2 \Phi \Theta \mathbf{V} \mathbf{s}_k \\ & \quad + \mathbf{A}_k \frac{1}{\sqrt{\tau p}} \mathbf{N} \mathbf{s}_k + (\mathbf{I}_M - \mathbf{A}_k) \eta \rho \sqrt{c_k \delta \varepsilon_k \bar{\mathbf{H}}_2 \Phi \bar{\mathbf{h}}_k}. \end{aligned} \quad (74)$$

With the definition of  $\sum_{w=1}^4 \mathbf{q}_k^w$ , we can get the expression of  $\hat{\mathbf{q}}_k$  as (16).

Utilizing the estimate  $\hat{\mathbf{q}}_k$ , we obtain the estimation error as  $\mathbf{e}_k = \mathbf{q}_k - \hat{\mathbf{q}}_k$  and the mean of  $\mathbf{e}_k$  is zero. As stated in [33], we calculate the MSE matrix as

$$\begin{aligned} & \mathbf{MSE}_k = \mathbb{E}\{\mathbf{e}_k \mathbf{e}_k^H\} \\ &= \text{Cov}\{\mathbf{q}_k, \mathbf{q}_k\} - \text{Cov}\{\mathbf{q}_k, \mathbf{y}_p^k\} \text{Cov}^{-1}\{\mathbf{y}_p^k, \mathbf{y}_p^k\} \text{Cov}\{\mathbf{y}_p^k, \mathbf{q}_k\} \\ &= (\mathbf{I}_M - \mathbf{A}_k) \text{Cov}\{\mathbf{q}_k, \mathbf{q}_k\} \\ & \triangleq a_{k5} \mathbf{a}_M \mathbf{a}_M^H + a_{k6} \mathbf{I}_M, \end{aligned} \quad (75)$$

where  $a_{k5} = \frac{a_{k1} \left( \frac{\sigma^2}{\tau p} + \varpi \right)^2 + M a_{k1} \varpi \delta \left( a_{k2} + \frac{\sigma^2}{\tau p} + \varpi \right) + \varpi \delta a_{k2}^2}{\left( a_{k2} + \frac{\sigma^2}{\tau p} + \varpi \right) \left( a_{k2} + \frac{\sigma^2}{\tau p} + \varpi + M (a_{k1} + \varpi \delta) \right)}$ , and

$$a_{k6} = \frac{a_{k2} \left( \frac{\sigma^2}{\tau p} + \varpi \right)}{a_{k2} + \frac{\sigma^2}{\tau p} + \varpi}.$$

Using the  $\mathbf{MSE}_k$  matrix, the  $\text{NMSE}_k$  is formulated as in [27]

$$\text{NMSE}_k = \frac{\text{Tr}\{\mathbf{MSE}_k\}}{\text{Tr}\{\text{Cov}\{\mathbf{q}_k, \mathbf{q}_k\}\}} = \frac{(a_{k5} + a_{k6})}{(a_{k1} + a_{k2})}. \quad (76)$$

$$E_k^{t\text{ nosie}}(\Phi) = \frac{\beta}{(\delta+1)} \left\{ (M^2 N \Delta \delta^2 e_{k2}^2 + MN \Delta \delta e_{k2}^2 + 2M^2 \Delta \delta e_{k1} e_{k2}) \left\{ c_k [\varepsilon_k (1 - \rho^2) + 1] + \frac{\varpi}{\Delta} \right\} + M^2 \Delta e_{k1}^2 c_k (\varepsilon_k + 1) \right. \\ \left. + \left\{ 2M^2 N \delta a_{k3} a_{k4} + MN (\delta a_{k4}^2 + e_{k3}) + M^3 N \delta a_{k3}^2 \right\} \left\{ \Delta c_k (\varepsilon_k + 1) + \varpi + \frac{\sigma^2}{\tau p} + \gamma_k \right\} + |f_k(\Phi)|^2 \Delta c_k \delta \varepsilon_k \rho^2 \left( M^2 \delta + 2 \frac{M^2}{N} e_{k1} + M \right) \right\}. \quad (87)$$

By substituting the values of  $m_k$  and  $n_k$  into (76), we obtain the specific expression of  $\text{NMSE}_k$ .

## APPENDIX D PROOF OF THEOREM 2

Before deriving the closed expression, we first give several useful results used in the following computations. Since  $\mathbf{A}_k \triangleq a_{k3} \mathbf{a}_M \mathbf{a}_M^H + a_{k4} \mathbf{I}_M$  and  $\bar{\mathbf{H}}_2 = \mathbf{a}_M \mathbf{a}_M^H$ , we can get that

$$\text{Tr} \{ \mathbf{A}_k \} = M (a_{k3} + a_{k4}) \triangleq M e_{k1}, \quad (77)$$

$$\mathbf{A}_k \bar{\mathbf{H}}_2 = a_{k3} \mathbf{a}_M \mathbf{a}_M^H \mathbf{a}_M \mathbf{a}_M^H + a_{k4} \mathbf{a}_M \mathbf{a}_M^H \\ = (M a_{k3} + a_{k4}) \bar{\mathbf{H}}_2 \triangleq e_{k2} \bar{\mathbf{H}}_2, \quad (78)$$

$$\text{Tr} \{ \mathbf{A}_k \mathbf{A}_k^H \} = \text{Tr} \{ M a_{k3}^2 \mathbf{a}_M \mathbf{a}_M^H + 2 a_{k3} a_{k4} \mathbf{a}_M \mathbf{a}_M^H + a_{k4}^2 \mathbf{I}_M \} \\ = M (M a_{k3}^2 + 2 a_{k3} a_{k4} + a_{k4}^2) \triangleq M e_{k3}, \quad (79)$$

where we define three auxiliary variables  $e_{k1}$ ,  $e_{k2}$ , and  $e_{k3}$ .

Then we focus on deriving each part in (28). Firstly, we introduce the derivation of the noise term which is divided into static noise at the BS and thermal noise at the active RIS. For clarity, we define that

$$E_k^{n\text{osie}}(\Phi) = \sigma^2 E_k^{s\text{nosie}}(\Phi) + \eta^2 \sigma_e^2 E_k^{t\text{nosie}}(\Phi). \quad (80)$$

Based on the orthogonality property of the LMMSE estimator, the observation vector  $\mathbf{y}_p^k$  is orthogonal to estimation error  $\mathbf{e}_k$ , i.e.,  $\mathbb{E} \{ \mathbf{y}_p^k \mathbf{e}_k \} = 0$ . Since  $\mathbb{E} \{ \mathbf{e}_k \} = 0$ , we have

$$\mathbb{E} \{ \hat{\mathbf{q}}_k^H \mathbf{q}_k \} = \mathbb{E} \{ \hat{\mathbf{q}}_k^H (\hat{\mathbf{q}}_k + \mathbf{e}_k) \} \\ = \mathbb{E} \{ \hat{\mathbf{q}}_k^H \hat{\mathbf{q}}_k \} + \mathbb{E} \{ (\mathbf{A}_k \mathbf{y}_p^k + \mathbf{B}_k)_k^H \mathbf{e}_k \} = \mathbb{E} \{ \|\hat{\mathbf{q}}_k\|^2 \}. \quad (81)$$

We denote the static noise term in the  $\text{SINR}_k$  as  $\mathbb{E} \{ \|\hat{\mathbf{q}}_k\|^2 \} \triangleq E_k^{s\text{nosie}}(\Phi)$ . Recalling the expressions of (8) and (16), we remove the zero-expectation terms in  $\mathbb{E} \{ \|\hat{\mathbf{q}}_k\|^2 \}$  and derive it as

$$E_k^{s\text{nosie}}(\Phi) = \mathbb{E} \{ \|\hat{\mathbf{q}}_k\|^2 \} = \mathbb{E} \{ \hat{\mathbf{q}}_k^H \mathbf{q}_k \} \\ = M \left\{ \Delta c_k \delta e_{k2} [\varepsilon_k (1 - \rho^2) + 1] + \Delta c_k (\varepsilon_k + 1) e_{k1} + \gamma_k e_{k1} \right\} \\ + \frac{M}{N} |f_k(\Phi)|^2 \Delta c_k \delta \varepsilon_k \rho^2. \quad (82)$$

In addition, we define the thermal noise term as  $E_k^{t\text{nosie}}(\Phi) \triangleq \mathbb{E} \{ \|\hat{\mathbf{q}}_k^H \mathbf{H}_2 \Phi \Theta\|^2 \}$ . By substituting  $\mathbf{H}_2 = \sqrt{\frac{\beta}{\delta+1}} (\sqrt{\delta} \bar{\mathbf{H}}_2 + \tilde{\mathbf{H}}_2)$  into the thermal noise term, we can

obtain

$$\mathbb{E} \left\{ \|\hat{\mathbf{q}}_k^H \mathbf{H}_2 \Phi \Theta\|^2 \right\} = \frac{\beta}{\delta+1} \left\{ \mathbb{E} \left\{ \hat{\mathbf{q}}_k^H \delta \bar{\mathbf{H}}_2 \bar{\mathbf{H}}_2^H \hat{\mathbf{q}}_k \right\} \right. \\ \left. + 2 \mathbb{E} \left\{ \hat{\mathbf{q}}_k^H \sqrt{\delta} \bar{\mathbf{H}}_2 \tilde{\mathbf{H}}_2^H \hat{\mathbf{q}}_k \right\} + \mathbb{E} \left\{ \hat{\mathbf{q}}_k^H \tilde{\mathbf{H}}_2 \tilde{\mathbf{H}}_2^H \hat{\mathbf{q}}_k \right\} \right\}. \quad (83)$$

Using Lemma 4 and the independence between  $\tilde{\mathbf{H}}_2$ ,  $\tilde{\mathbf{h}}_k$ ,  $\tilde{\mathbf{d}}_k$  and  $\mathbf{N}$ , the specific expression of each term in  $E_k^{t\text{nosie}}(\Phi)$  is calculated respectively as

$$\mathbb{E} \left\{ \hat{\mathbf{q}}_k^H \delta \bar{\mathbf{H}}_2 \bar{\mathbf{H}}_2^H \hat{\mathbf{q}}_k \right\} \\ = M^2 \Delta |f_k(\Phi)|^2 c_k \delta^2 \varepsilon_k \rho^2 \\ + M^2 N \Delta \delta^2 e_{k2}^2 \left\{ c_k [\varepsilon_k (1 - \rho^2) + 1] + \frac{\varpi}{\Delta} \right\} \\ + MN \delta (a_{k3} M + a_{k4})^2 \left\{ \Delta c_k (\varepsilon_k + 1) + \varpi + \frac{\sigma^2}{\tau p} + \gamma_k \right\}, \quad (84)$$

$$2 \mathbb{E} \left\{ \hat{\mathbf{q}}_k^H \sqrt{\delta} \bar{\mathbf{H}}_2 \tilde{\mathbf{H}}_2^H \hat{\mathbf{q}}_k \right\} \\ = 2 \frac{M^2}{N} |f_k(\Phi)|^2 \Delta \rho^2 c_k \delta \varepsilon_k e_{k1} \\ + 2 M^2 \Delta \delta e_{k1} e_{k2} \left\{ c_k [\varepsilon_k (1 - \rho^2) + 1] + \frac{\varpi}{\Delta} \right\}, \quad (85)$$

$$\mathbb{E} \left\{ \hat{\mathbf{q}}_k^H \tilde{\mathbf{H}}_2 \tilde{\mathbf{H}}_2^H \hat{\mathbf{q}}_k \right\} \\ = M |f_k(\Phi)|^2 \Delta c_k \delta \varepsilon_k \rho^2 + M^2 \Delta c_k (\varepsilon_k + 1) e_{k1} \\ + MN \left\{ \Delta \delta e_{k2}^2 \left\{ \frac{\varpi}{\Delta} + c_k [\varepsilon_k (1 - \rho^2) + 1] \right\} \right. \\ \left. + e_{k3} \left\{ \gamma_k + \frac{\sigma^2}{\tau p} + \varpi + \Delta c_k (\varepsilon_k + 1) \right\} \right\}. \quad (86)$$

As a result, we can get the expression of  $E_k^{t\text{nosie}}(\Phi)$  as (87) at the top of this page. Finally, we can obtain the noise term in (80). Based on (82) and (87),  $E_k^{n\text{osie}}(\Phi)$  is calculated as (88) at the bottom of this page.

To the desired signal term, we denote it as  $E_k^{s\text{signal}}(\Phi)$ . From the procedure for obtaining  $E_k^{s\text{nosie}}(\Phi)$ , we have known that  $\mathbb{E} \{ \hat{\mathbf{q}}_k \mathbf{q}_k \}$  is a real variable, then we calculate it as

$$E_k^{s\text{signal}}(\Phi) = |\mathbb{E} \{ \hat{\mathbf{q}}_k^H \mathbf{q}_k \}|^2 = \left( \mathbb{E} \{ \|\hat{\mathbf{q}}_k\|^2 \} \right)^2, \quad (89)$$

and the specific expression of  $E_k^{s\text{signal}}(\Phi)$  is given as (90) at the top of the next page.

$$E_k^{n\text{osie}}(\Phi) = \sigma^2 E_k^{s\text{nosie}}(\Phi) + \eta^2 \sigma_e^2 E_k^{t\text{nosie}}(\Phi) \\ = \sigma^2 M \left\{ \Delta c_k \delta e_{k2} [\varepsilon_k (1 - \rho^2) + 1] + \Delta c_k (\varepsilon_k + 1) e_{k1} + \gamma_k e_{k1} \right\} + \sigma^2 \frac{M}{N} |f_k(\Phi)|^2 \Delta c_k \delta \varepsilon_k \rho^2 \\ + \frac{\sigma_e^2 \Delta \beta}{N(\delta+1)} \left\{ (M^2 N \Delta \delta^2 e_{k2}^2 + MN \Delta \delta e_{k2}^2 + 2M^2 \Delta \delta e_{k1} e_{k2}) \left\{ c_k [\varepsilon_k (1 - \rho^2) + 1] + \frac{\varpi}{\Delta} \right\} + M^2 \Delta e_{k1}^2 c_k (\varepsilon_k + 1) \right. \\ \left. + \left\{ 2M^2 N \delta a_{k3} a_{k4} + MN (\delta a_{k4}^2 + e_{k3}) + M^3 N \delta a_{k3}^2 \right\} \left\{ \Delta c_k (\varepsilon_k + 1) + \varpi + \frac{\sigma^2}{\tau p} + \gamma_k \right\} + |f_k(\Phi)|^2 \Delta c_k \delta \varepsilon_k \rho^2 \left( M^2 \delta + 2 \frac{M^2}{N} e_{k1} + M \right) \right\}. \quad (88)$$

$$\begin{aligned}
E_k^{signal}(\Phi) &= M^2 \{ \Delta c_k \delta e_{k2} [\varepsilon_k (1-\rho^2) + 1] + \Delta c_k (\varepsilon_k + 1) e_{k1} + \gamma_k e_{k1} \}^2 + \frac{M^2}{N^2} |f_k(\Phi)|^4 \Delta^2 c_k^2 \delta^2 \varepsilon_k^2 \rho^4 \\
&\quad + 2 \frac{M^2}{N} |f_k(\Phi)|^2 \Delta c_k \delta \varepsilon_k \rho^2 \{ \Delta c_k \delta e_{k2} [\varepsilon_k (1-\rho^2) + 1] + \Delta c_k (\varepsilon_k + 1) e_{k1} + \gamma_k e_{k1} \}^2. \tag{90}
\end{aligned}$$

After that, we compute the interference term  $\mathbb{E} \{ |\hat{\mathbf{q}}_k^H \mathbf{q}_i|^2 \}$  which is denoted as  $I_{ki}(\Phi)$ . Recalling the expressions of  $\hat{\mathbf{q}}_k^H$  and  $\mathbf{q}_i$ , we decompose  $I_{ki}(\Phi)$  as

$$\begin{aligned}
I_{ki}(\Phi) &= \mathbb{E} \{ |\hat{\mathbf{q}}_k^H \mathbf{q}_i|^2 \} = \mathbb{E} \left\{ \left| \frac{\hat{\mathbf{q}}_k^H \mathbf{q}_i}{\sqrt{\tau p}} \right|^2 \right\} + \mathbb{E} \left\{ \left| \frac{\hat{\mathbf{q}}_k^H \mathbf{d}_i}{\sqrt{\tau p}} \right|^2 \right\} \\
&\quad + \mathbb{E} \left\{ \left| \left( \frac{\eta}{\sqrt{\tau p}} \mathbf{A}_k \mathbf{H}_2 \Phi \Theta \mathbf{V} \mathbf{s}_k \right)^H \mathbf{q}_i \right|^2 \right\} \\
&\quad + \mathbb{E} \left\{ \left| \left( \frac{\eta}{\sqrt{\tau p}} \mathbf{A}_k \mathbf{H}_2 \Phi \Theta \mathbf{V} \mathbf{s}_k \right)^H \mathbf{d}_i \right|^2 \right\} \\
&\quad + \mathbb{E} \left\{ \left| \left( \frac{1}{\sqrt{\tau p}} \mathbf{A}_k \mathbf{N} \mathbf{s}_k \right)^H \mathbf{q}_i \right|^2 \right\} + \mathbb{E} \left\{ \left| \left( \frac{1}{\sqrt{\tau p}} \mathbf{A}_k \mathbf{N} \mathbf{s}_k \right)^H \mathbf{d}_i \right|^2 \right\} \\
&\quad + \mathbb{E} \left\{ \left| (\mathbf{A}_k \mathbf{d}_k)^H \mathbf{q}_i \right|^2 \right\} + \mathbb{E} \left\{ \left| (\mathbf{A}_k \mathbf{d}_k)^H \mathbf{d}_i \right|^2 \right\}. \tag{91}
\end{aligned}$$

Then, we calculate the last seven expectations directly as

$$\mathbb{E} \left\{ \left| (\mathbf{A}_k \mathbf{d}_k)^H \mathbf{d}_i \right|^2 \right\} = \gamma_k \gamma_i M e_{k3}, \tag{92}$$

$$\begin{aligned}
\mathbb{E} \left\{ \left| (\mathbf{A}_k \mathbf{d}_k)^H \mathbf{q}_i \right|^2 \right\} &= \frac{M}{N} |f_i(\Phi)|^2 \Delta c_i \delta \varepsilon_i e_{k2}^2 \rho^2 \gamma_k \\
&\quad + \Delta M c_i \gamma_k \{ \delta e_{k2}^2 [\varepsilon_i (1-\rho^2) + 1] + (\varepsilon_i + 1) e_{k3} \}, \tag{93}
\end{aligned}$$

$$\mathbb{E} \left\{ \left| \left( \frac{1}{\sqrt{\tau p}} \mathbf{A}_k \mathbf{N} \mathbf{s}_k \right)^H \mathbf{d}_i \right|^2 \right\} = \frac{\sigma^2}{\tau p} \gamma_i M e_{k3}, \tag{94}$$

$$\begin{aligned}
\mathbb{E} \left\{ \left| \left( \frac{1}{\sqrt{\tau p}} \mathbf{A}_k \mathbf{N} \mathbf{s}_k \right)^H \mathbf{q}_i \right|^2 \right\} &= \frac{M}{N} |f_i(\Phi)|^2 \Delta c_i \delta \varepsilon_i e_{k2}^2 \rho^2 \frac{\sigma^2}{\tau p} \\
&\quad + \Delta M c_i \frac{\sigma^2}{\tau p} \{ \delta e_{k2}^2 [\varepsilon_i (1-\rho^2) + 1] + (\varepsilon_i + 1) e_{k3} \}, \tag{95}
\end{aligned}$$

$$\mathbb{E} \left\{ \left| \left( \frac{\eta}{\sqrt{\tau p}} \mathbf{A}_k \mathbf{H}_2 \Phi \Theta \mathbf{V} \mathbf{s}_k \right)^H \mathbf{d}_i \right|^2 \right\} = M \varpi \gamma_i (\delta e_{k2}^2 + e_{k3}), \tag{96}$$

$$\begin{aligned}
&\mathbb{E} \left\{ \left| \left( \frac{\eta}{\sqrt{\tau p}} \mathbf{A}_k \mathbf{H}_2 \Phi \Theta \mathbf{V} \mathbf{s}_k \right)^H \mathbf{q}_i \right|^2 \right\} \\
&= \Delta \varpi \left\{ \frac{M}{N} |f_i(\Phi)|^2 c_i \delta \varepsilon_i \rho^2 e_{k2}^2 \right. \\
&\quad + \frac{M}{N} |f_i(\Phi)|^2 c_i \delta \varepsilon_i \rho^2 e_{k2}^2 + M c_i \delta^2 e_{k2}^2 \{ \varepsilon_i (1-\rho^2) + 1 \} \\
&\quad + \frac{M^2}{N} |f_i(\Phi)|^2 c_i \delta^2 \varepsilon_i \rho^2 e_{k2}^2 + \frac{2M^2}{N^2} |f_i(\Phi)|^2 c_i \delta \varepsilon_i \rho^2 e_k e_{k2} \\
&\quad + \frac{M^2}{N} c_i \{ 2\delta e_{k1} e_{k2} [\varepsilon_i (1-\rho^2) + 1] + (\varepsilon_i + 1) e_{k1}^2 \} \\
&\quad \left. + M c_i \{ (2\varepsilon_i + 2 - \varepsilon_i \rho^2) \delta e_{k2}^2 + (\varepsilon_i + 1) e_{k3} \} \right\}, \tag{97}
\end{aligned}$$

$$\begin{aligned}
\mathbb{E} \left\{ \left| \hat{\mathbf{q}}_k^H \mathbf{d}_i \right|^2 \right\} &= \frac{M}{N} |f_k(\Phi)|^2 \Delta \gamma_i c_k \delta \varepsilon_k \rho^2 \\
&\quad + M \Delta \gamma_i c_k \{ \delta e_{k2}^2 [\varepsilon_k (1-\rho^2) + 1] + (\varepsilon_k + 1) e_{k3} \}. \tag{98}
\end{aligned}$$

However, for the first term in (91), we proceed by expand-

ing its expression as

$$\begin{aligned}
\mathbb{E} \left\{ \left| \hat{\mathbf{q}}_k^H \mathbf{q}_i \right|^2 \right\} &= \mathbb{E} \left\{ \left| \sum_{w=1}^6 (\hat{\mathbf{q}}_k^w)^H \sum_{\psi=1}^4 \mathbf{q}_i^\psi \right|^2 \right\} \\
&= \sum_{w=1}^6 \sum_{\psi=1}^4 \mathbb{E} \left\{ \left| (\hat{\mathbf{q}}_k^w)^H \mathbf{q}_i^\psi \right|^2 \right\} \\
&\quad + \sum_{(w_1, \psi_1) \neq (w_2, \psi_2)} \mathbb{E} \left\{ \left( (\hat{\mathbf{q}}_k^{w_1})^H (\mathbf{q}_i^{\psi_1}) \right) \left( (\hat{\mathbf{q}}_k^{w_2})^H (\mathbf{q}_i^{\psi_2}) \right)^H \right\}. \tag{99}
\end{aligned}$$

Similar to the process described above for calculating other terms, we utilize the independence between random variables and Lemma 4 to compute the modulus-square terms and cross-terms in (99).

Firstly, we compute one of the 24 modulus-square terms. When  $w = 1$  and  $\psi = 1$ , we have

$$\begin{aligned}
\mathbb{E} \left\{ \left| (\hat{\mathbf{q}}_k^1)^H \mathbf{q}_i^1 \right|^2 \right\} &= \Delta^2 c_k \delta^2 \varepsilon_k c_i \varepsilon_i e_{k2}^2 \left\{ \frac{M^2}{N^2} \bar{\mathbf{h}}_i^H \bar{\mathbf{h}}_k |2(1-\rho^2)|^2 \right. \\
&\quad + \frac{M^2}{N^2} |F_{ki}|^2 (1-\rho^2)^2 + \frac{M^2}{N} (|f_i(\Phi)|^2 + |f_k(\Phi)|^2) \rho^2 (1-\rho^2) \\
&\quad + \frac{M^2}{N^2} (|f_i(\Phi)|^2 + |f_k(\Phi)|^2) 2\rho^2 (2\rho^2 - 1 - l) + M^2 (1-\rho^2)^2 \\
&\quad + \frac{M^2}{N} (4\rho^2 + 4l\rho^2 - l^2 - 1 - 6\rho^4) + \frac{M^2}{N^2} |f_i(\Phi)|^2 |f_i(\Phi)|^2 \rho^4 \\
&\quad + 2 \frac{M^2}{N^2} \text{Re} \left\{ \bar{\mathbf{h}}_i^H \bar{\mathbf{h}}_i f_i^H(\Phi) f_k(\Phi) \right\} \rho^2 (1-\rho^2) \\
&\quad \left. + 2 \frac{M^2}{N^2} \text{Re} \left\{ F_{ki}^H f_k(\Phi) f_i(\Phi) \right\} \rho^2 (1-\rho^2) \right\}. \tag{100}
\end{aligned}$$

When  $w = 1$ , the remaining terms can be calculated as

$$\begin{aligned}
\sum_{\psi=2}^4 \mathbb{E} \left\{ \left| (\hat{\mathbf{q}}_k^1)^H \mathbf{q}_i^\psi \right|^2 \right\} &= \eta^4 c_k \delta \varepsilon_k c_i e_{k2}^2 M N \\
&\quad \times \{ \rho^2 |f_k(\Phi)|^2 + (1-\rho^2) N \} \{ \delta M + \varepsilon_i + 1 \}. \tag{101}
\end{aligned}$$

Likewise, when  $w = 2, 3, 4, 5, 6$ , we get other modulus-square terms as

$$\begin{aligned}
\sum_{\psi=1}^4 \mathbb{E} \left\{ \left| (\hat{\mathbf{q}}_k^2)^H \mathbf{q}_i^\psi \right|^2 \right\} &= \eta^4 c_k \delta c_i e_{k2}^2 M N^2 \{ \delta M + \varepsilon_i + 1 \} \\
&\quad + \eta^4 c_k \delta c_i \varepsilon_i e_{k2}^2 M^2 N \{ \rho^2 |f_i(\Phi)|^2 + (1-\rho^2) N \}, \tag{102}
\end{aligned}$$

$$\begin{aligned}
\sum_{\psi=1}^4 \mathbb{E} \left\{ \left| (\hat{\mathbf{q}}_k^3)^H \mathbf{q}_i^\psi \right|^2 \right\} &= \eta^4 c_k \varepsilon_k c_i \delta e_{k2}^2 M N^2 \\
&\quad + \eta^4 c_k \varepsilon_k c_i \varepsilon_i \delta e_{k2}^2 M N \{ \rho^2 |f_i(\Phi)|^2 + (1-\rho^2) N \} \\
&\quad + \eta^4 c_k \varepsilon_k c_i \varepsilon_i \left\{ e_{k1}^2 M^2 \bar{\mathbf{h}}_i^H \bar{\mathbf{h}}_k |2 + e_{k3} M N^2 \right\} \\
&\quad + \eta^4 c_k \varepsilon_k c_i \left\{ e_{k1}^2 M^2 N + e_{k3} M N^2 \right\}, \tag{103}
\end{aligned}$$

$$\begin{aligned} & \sum_{\psi=1}^4 \mathbb{E} \left\{ \left| (\hat{\mathbf{q}}_k^4)^H \mathbf{q}_i^\psi \right|^2 \right\} = \eta^4 c_k c_i \delta e_{k2}^2 M N^2 \\ & + \eta^4 c_k c_i \delta \varepsilon_i e_{k2}^2 M N \left\{ \rho^2 |f_i(\Phi)|^2 + (1 - \rho^2) N \right\} \\ & + \eta^4 c_k c_i (\varepsilon_i + 1) N \left\{ e_{k1}^2 M^2 + e_{k3} M N \right\}, \end{aligned} \quad (104)$$

$$\begin{aligned} & \sum_{\psi=1}^4 \mathbb{E} \left\{ \left| (\hat{\mathbf{q}}_k^5)^H \mathbf{q}_i^\psi \right|^2 \right\} \\ & = \eta^4 \rho^2 c_k \varepsilon_k c_i \varepsilon_i \delta^2 M^2 |f_k(\Phi)|^2 \left\{ \rho^2 |f_i(\Phi)|^2 + (1 - \rho^2) N \right\} \\ & + \eta^4 \rho^2 c_k \delta \varepsilon_k c_i M N |f_k(\Phi)|^2 \left\{ \delta M + \varepsilon_i + 1 \right\}, \end{aligned} \quad (105)$$

$$\begin{aligned} & \sum_{\psi=1}^4 \mathbb{E} \left\{ \left| (\hat{\mathbf{q}}_k^6)^H \mathbf{q}_i^\psi \right|^2 \right\} \\ & = \sum_{\psi=1}^4 \mathbb{E} \left\{ \left| \left( -\eta \rho \sqrt{c_k \delta \varepsilon_k} \mathbf{A}_k \bar{\mathbf{H}}_2 \Phi \bar{\mathbf{h}}_k \right)^H \mathbf{q}_i^\psi \right|^2 \right\} \\ & = \eta^4 e_{k2}^2 \rho^2 c_k \varepsilon_k c_i \varepsilon_i \delta^2 M^2 |f_k(\Phi)|^2 \left\{ \rho^2 |f_i(\Phi)|^2 + (1 - \rho^2) N \right\} \\ & + \eta^4 e_{k2}^2 \rho^2 c_k \delta \varepsilon_k c_i M N |f_k(\Phi)|^2 \left\{ \delta M + \varepsilon_i + 1 \right\}, \end{aligned} \quad (106)$$

Additionally, although there is a total of 40 non-zero terms in the cross-terms, half of them are complex conjugates of the other half. Hence, we only need to calculate 20 non-zero terms. As a result, we have

$$\begin{aligned} & \sum_{(w_1, \psi_1) \neq (w_2, \psi_2)} \mathbb{E} \left\{ \left( (\hat{\mathbf{q}}_k^{w_1})^H (\mathbf{q}_i^{\psi_1}) \right) \left( (\hat{\mathbf{q}}_k^{w_2})^H (\mathbf{q}_i^{\psi_2}) \right)^H \right\} \\ & = 2 \operatorname{Re} \left\{ \sum_{w_1, \psi_1, w_2, \psi_2} \mathbb{E} \left\{ \left( (\hat{\mathbf{q}}_k^{w_1})^H (\mathbf{q}_i^{\psi_1}) \right) \left( (\hat{\mathbf{q}}_k^{w_2})^H (\mathbf{q}_i^{\psi_2}) \right)^H \right\} \right\}. \end{aligned} \quad (107)$$

Herein, we use  $\text{CS}_{ki}$  to represent the sum of all these cross-terms. Then, we calculate these non-zero terms one by one in (107) and we get (108) at the bottom of this page.

Finally, we can complete the derivation of  $I_{ki}(\Phi)$  with some simplifications. We express it as (109) which is shown at the top of the next page. In addition, during the calculation process, we define some phase shifts related variables as below

$$f_k(\Phi) \triangleq \mathbf{a}_N^H \Phi \bar{\mathbf{h}}_k \triangleq \sum_{n=1}^N f_{k,n}(\Phi) = \sum_{n=1}^N e^{j(\xi_n^k + \theta_n)}, \quad (110)$$

$$\begin{aligned} \xi_n^k &= 2\pi \frac{d}{\lambda} \left( \lfloor (n-1)/\sqrt{N} \rfloor (\sin \varphi_{\text{kr}}^a \sin \varphi_{\text{kr}}^e - \sin \varphi_{\text{t}}^a \sin \varphi_{\text{t}}^e) \right. \\ & \left. + \left( (n-1) \bmod \sqrt{N} \right) (\cos \varphi_{\text{kr}}^e - \cos \varphi_{\text{t}}^e) \right), \end{aligned} \quad (111)$$

$$F_{ki} \triangleq \sum_{n=1}^N f_{k,n}(\Phi) f_{i,n}(\Phi). \quad (112)$$

Following that, we calculate the signal leakage term which can be expressed as

$$E_k^{\text{leak}}(\Phi) = \mathbb{E} \left\{ \left| \hat{\mathbf{q}}_k^H \mathbf{q}_k \right|^2 \right\} - \left| \mathbb{E} \left\{ \hat{\mathbf{q}}_k^H \mathbf{q}_k \right\} \right|^2, \quad (113)$$

where  $\mathbb{E} \left\{ \hat{\mathbf{q}}_k^H \mathbf{q}_k \right\}$  is known as (82). Therefore, we only need to derive the expectation of  $\mathbb{E} \left\{ \left| \hat{\mathbf{q}}_k^H \mathbf{q}_k \right|^2 \right\}$ . Similar to the calculation of  $I_{ki}(\Phi)$ , we eliminate terms with zero expectation by utilizing the independence between the direct channel, the cascaded channel, and two kinds of noise. Finally,  $\mathbb{E} \left\{ \left| \hat{\mathbf{q}}_k^H \mathbf{q}_k \right|^2 \right\}$  can be expanded as

$$\begin{aligned} \mathbb{E} \left\{ \left| \hat{\mathbf{q}}_k^H \mathbf{q}_k \right|^2 \right\} &= \mathbb{E} \left\{ \left| \hat{\mathbf{q}}_k^H \underline{\mathbf{q}}_k \right|^2 \right\} + \mathbb{E} \left\{ \left| \hat{\mathbf{q}}_k^H \mathbf{d}_k \right|^2 \right\} \\ &+ \mathbb{E} \left\{ \left| \left( \frac{\eta}{\sqrt{\tau p}} \mathbf{A}_k \mathbf{H}_2 \Phi \mathbf{V} \mathbf{s}_k \right)^H \underline{\mathbf{q}}_k \right|^2 \right\} \\ &+ \mathbb{E} \left\{ \left| \left( \frac{\eta}{\sqrt{\tau p}} \mathbf{A}_k \mathbf{H}_2 \Phi \mathbf{V} \mathbf{s}_k \right)^H \mathbf{d}_k \right|^2 \right\} \\ &+ \mathbb{E} \left\{ \left| \left( \frac{1}{\sqrt{\tau p}} \mathbf{A}_k \mathbf{N} \mathbf{s}_k \right)^H \underline{\mathbf{q}}_k \right|^2 \right\} + \mathbb{E} \left\{ \left| \left( \frac{1}{\sqrt{\tau p}} \mathbf{A}_k \mathbf{N} \mathbf{s}_k \right)^H \mathbf{d}_k \right|^2 \right\} \\ &+ \mathbb{E} \left\{ \left| \left( \mathbf{A}_k \mathbf{d}_k \right)^H \underline{\mathbf{q}}_k \right|^2 \right\} + \mathbb{E} \left\{ \left| \left( \mathbf{A}_k \mathbf{d}_k \right)^H \mathbf{d}_k \right|^2 \right\} \\ &+ 2 \operatorname{Re} \left\{ \mathbb{E} \left\{ \left| \hat{\mathbf{q}}_k^H \underline{\mathbf{q}}_k \mathbf{d}_k^H \mathbf{A}_k \mathbf{d}_k \right|^2 \right\} \right\}. \end{aligned} \quad (114)$$

For the calculation of  $\mathbb{E} \left\{ \left| \hat{\mathbf{q}}_k^H \mathbf{q}_k \right|^2 \right\}$ , we omit the computation process of the last eight terms as they are straightforward and simple. Particularly, our main task is to compute the first term among the nine expectations. For the first term, we also expand it as

$$\begin{aligned} \mathbb{E} \left\{ \left| \hat{\mathbf{q}}_k^H \underline{\mathbf{q}}_k \right|^2 \right\} &= \mathbb{E} \left\{ \left| \sum_{w=1}^6 (\hat{\mathbf{q}}_k^w)^H \sum_{\psi=1}^4 \mathbf{q}_k^\psi \right|^2 \right\} \\ &= \sum_{w=1}^6 \sum_{\psi=1}^4 \mathbb{E} \left\{ \left| (\hat{\mathbf{q}}_k^w)^H \mathbf{q}_k^\psi \right|^2 \right\} \\ &+ \sum_{(w_1, \psi_1) \neq (w_2, \psi_2)} \mathbb{E} \left\{ \left( (\hat{\mathbf{q}}_k^{w_1})^H (\mathbf{q}_k^{\psi_1}) \right) \left( (\hat{\mathbf{q}}_k^{w_2})^H (\mathbf{q}_k^{\psi_2}) \right)^H \right\}. \end{aligned} \quad (115)$$

There are 24 modulus-square terms and 64 non-zero cross-terms. Similarly, half of cross-terms are complex conjugates of the other half. As the derivation process of the interference term, we calculate the expectations of non-zero terms. Finally, the expression of  $E_k^{\text{leak}}(\Phi)$  is presented as (116) at the top of the next page.

## REFERENCES

- [1] Q. Wu and R. Zhang, "Intelligent reflecting surface enhanced wireless network via joint active and passive beamforming," *IEEE Trans. Wireless Commun.*, vol. 18, no. 11, pp. 5394–5409, Nov. 2019.
- [2] Q. Tao, J. Wang, and C. Zhong, "Performance analysis of intelligent reflecting surface aided communication systems," *IEEE Commun. Lett.*, vol. 24, no. 11, pp. 2464–2468, Nov. 2020.

$$\begin{aligned} \text{CS}_{ki} &= 2\eta^4 c_k \varepsilon_k \delta c_i \varepsilon_i e_{k1} e_{k2} M^2 \operatorname{Re} \left\{ \rho^2 f_i(\Phi) f_k^H(\Phi) \bar{\mathbf{h}}_i^H \bar{\mathbf{h}}_k + (1 - \rho^2) |\bar{\mathbf{h}}_k^H \bar{\mathbf{h}}_i|^2 \right\} + 2\eta^4 c_k \delta c_i e_{k1} e_{k2} M^2 N + 2\eta^4 \rho^2 c_k \delta \varepsilon_k c_i e_{k1} M^2 |f_k(\Phi)|^2 (1 - e_{k2}) \\ &+ 2\eta^4 M^2 \operatorname{Re} \left\{ \bar{\mathbf{h}}_k^H \bar{\mathbf{h}}_i f_i^H(\Phi) f_k(\Phi) \right\} \left\{ \rho^2 (1 - \rho^2) c_k \delta^2 \varepsilon_k c_i \varepsilon_i e_{k2} (1 - e_{k2}) \right\} + 2\eta^4 M^2 \operatorname{Re} \left\{ F_{ki}^H f_i(\Phi) f_k(\Phi) \right\} \left\{ \rho^2 (1 - \rho^2) c_k \delta^2 \varepsilon_k c_i \varepsilon_i e_{k2} (1 - e_{k2}) \right\} \\ &+ 2\eta^4 M^2 |f_k(\Phi)|^2 \rho^2 c_k \delta^2 \varepsilon_k c_i \varepsilon_i e_{k2} (1 - e_{k2}) (2\rho^2 - l - 1) + 2\eta^4 M^2 N |f_k(\Phi)|^2 \Delta^2 \rho^2 (1 - \rho^2) c_k \delta^2 \varepsilon_k c_i \varepsilon_i e_{k2} (1 - e_{k2}) \\ &+ 2\eta^4 M^2 |f_k(\Phi)|^2 |f_i(\Phi)|^2 \rho^4 c_k \delta^2 \varepsilon_k c_i \varepsilon_i e_{k2} (1 - e_{k2}) + 2\eta^4 c_k \delta \varepsilon_k c_i e_{k1} e_{k2} M^2 \left\{ \rho^2 |f_k(\Phi)|^2 + (1 - \rho^2) N \right\} + 2\eta^4 c_k \delta c_i \varepsilon_i e_{k1} e_{k2} M^2 \left\{ \rho^2 |f_i(\Phi)|^2 + (1 - \rho^2) N \right\} \\ &+ 2\eta^4 \rho^2 c_k \delta \varepsilon_k c_i e_{k2} M N |f_k(\Phi)|^2 (1 - e_{k2}) (\delta M + \varepsilon_i + 1) + 2\eta^4 \rho^2 c_k \delta \varepsilon_k c_i \varepsilon_i e_{k1} M^2 \operatorname{Re} \left\{ \bar{\mathbf{h}}_k^H \bar{\mathbf{h}}_i f_i^H(\Phi) f_k(\Phi) \right\} (1 - e_{k2}) \\ &- 2\eta^4 \rho^2 c_k \delta^2 \varepsilon_k c_i \varepsilon_i e_{k2} M^2 |f_k(\Phi)|^2 \left\{ \rho^2 |f_i(\Phi)|^2 + (1 - \rho^2) N \right\} - 2\eta^4 \rho^2 c_k \delta \varepsilon_k c_i e_{k2} M N |f_k(\Phi)|^2 (\delta M + \varepsilon_i + 1). \end{aligned} \quad (108)$$

$$\begin{aligned}
I_{ki}(\Phi) &= \frac{M^2}{N^2} |\bar{\mathbf{h}}_k^H \bar{\mathbf{h}}_i|^2 \Delta^2 c_k \varepsilon_k c_i \varepsilon_i [\delta e_{k2}(1-\rho^2) + e_{k1}]^2 + \frac{M^2}{N^2} |F_{ki}|^2 \Delta^2 c_k \delta^2 \varepsilon_k c_i \varepsilon_i e_{k2}^2 (l-\rho^2)^2 + \frac{M^2}{N^2} |f_k(\Phi)|^2 |f_i(\Phi)|^2 \Delta^2 \rho^4 c_k \delta^2 \varepsilon_k c_i \varepsilon_i \\
&+ 2 \frac{M^2}{N^2} \Delta^2 \rho^2 c_i \delta \left\{ c_k \delta \varepsilon_k \varepsilon_i e_{k2} (2\rho^2 - 1 - l) \left\{ |f_k(\Phi)|^2 + |f_i(\Phi)|^2 e_{k2} \right\} + |f_k(\Phi)|^2 c_k \varepsilon_k e_{k1} + |f_i(\Phi)|^2 \varepsilon_i e_{k1} e_{k2} \left( c_k + \frac{\varpi}{\Delta} \right) \right\} \\
&+ \frac{M^2}{N} \Delta^2 \rho^2 c_i \delta^2 \left\{ c_k \varepsilon_k \varepsilon_i (1-\rho^2) \left\{ |f_k(\Phi)|^2 + |f_i(\Phi)|^2 e_{k2}^2 \right\} + |f_k(\Phi)|^2 c_k \varepsilon_k + |f_i(\Phi)|^2 \varepsilon_i e_{k2}^2 \left( c_k + \frac{\varpi}{\Delta} \right) \right\} \\
&+ \frac{M}{N} \Delta \rho^2 \delta \left\{ \Delta c_k \varepsilon_k c_i \varepsilon_i \left\{ |f_k(\Phi)|^2 + |f_i(\Phi)|^2 e_{k2}^2 \right\} + c_k \varepsilon_k |f_k(\Phi)|^2 (\Delta c_i + \gamma_i) + |f_i(\Phi)|^2 c_i \varepsilon_i e_{k2}^2 \left( \frac{\sigma^2}{\tau p} + \varpi + \gamma_k + \Delta c_k \right) \right\} \\
&+ M^2 \Delta^2 c_i \delta^2 e_{k2}^2 \left\{ c_k (1-\rho^2) \left\{ \varepsilon_i + \varepsilon_k + \varepsilon_i \varepsilon_k (1-\rho^2) \right\} + c_k + \frac{\varpi}{\Delta} \left\{ 1 + \varepsilon_i (1-\rho^2) \right\} \right\} + \frac{M^2}{N} \Delta^2 c_i e_{k1} \left( c_k + \frac{\varpi}{\Delta} \right) (2\delta e_{k2} + e_{k1}) \\
&+ \frac{M^2}{N} \Delta^2 c_i \left\{ c_k \varepsilon_k \delta^2 \varepsilon_i e_{k2}^2 (4\rho^2 + 4l\rho^2 - l^2 - 1 - 6\rho^4) + e_{k1} \left\{ \varepsilon_i \left( c_k + \frac{\varpi}{\Delta} \right) + c_k \varepsilon_k \right\} \left\{ 2\delta e_{k2} (1-\rho^2) + e_{k1} \right\} \right\} \\
&+ M \left\{ \Delta^2 c_k c_i \left\{ (\varepsilon_k \varepsilon_i + \varepsilon_k + \varepsilon_i + 1) (2\delta e_{k2}^2 + e_{k3}) - \rho^2 \delta e_{k2}^2 (2\varepsilon_k \varepsilon_i + \varepsilon_k + \varepsilon_i) \right\} + \varpi \left\{ (\delta e_{k2}^2 + e_{k3}) \gamma_i + \Delta c_i (\varepsilon_i + 1) (2\delta e_{k2}^2 + e_{k3}) - \Delta \delta e_{k2}^2 c_i \varepsilon_i \rho^2 \right\} \right. \\
&+ \left. \left( \frac{\sigma^2}{\tau p} + \gamma_k \right) \left\{ \Delta c_i (\varepsilon_i + 1) (\delta e_{k2}^2 + e_{k3}) - \Delta \delta e_{k2}^2 c_i \varepsilon_i \rho^2 + e_{k3} \gamma_i \right\} + \Delta c_k \gamma_i (\varepsilon_k + 1) (\delta e_{k2}^2 + e_{k3}) - \Delta \delta e_{k2}^2 c_k \gamma_i \varepsilon_k \rho^2 \right\} \\
&+ 2 \frac{M^2}{N^2} \text{Re} \left\{ \bar{\mathbf{h}}_k^H \bar{\mathbf{h}}_i F_i^H(\Phi) f_k(\Phi) \right\} \Delta^2 \rho^2 c_k \delta \varepsilon_k c_i \varepsilon_i \left\{ \delta e_{k2} (1-\rho^2) + e_{k1} \right\} + 2 \frac{M^2}{N^2} \text{Re} \left\{ F_{ki}^H f_k(\Phi) f_i(\Phi) \right\} \Delta^2 \rho^2 (l-\rho^2) c_k \delta^2 \varepsilon_k c_i \varepsilon_i e_{k2}. \quad (109)
\end{aligned}$$

$$\begin{aligned}
E_k^{leak}(\Phi) &= M^2 \Delta^2 \left\{ c_k \delta^2 e_{k2}^2 [\varepsilon_k (1-\rho^2) + 1] \left\{ c_k [\varepsilon_k (1-\rho^2) + 1] + \frac{\varpi}{\Delta} \right\} + 2c_k^2 \delta e_{k1} e_{k2} (e_{k2} - 1) \right\} + 2 \frac{M}{N^2} |f_k(\Phi)|^2 \Delta^2 \rho^2 c_k^2 \delta \varepsilon_k e_{k2} (1 + e_{k2}) \\
&+ \frac{M^2}{N} \Delta^2 c_k \left\{ e_{k1} \left\{ \varepsilon_k (2c_k + \frac{\varpi}{\Delta}) [2\delta e_{k2} (1-\rho^2) + e_{k1}] + e_{k1} (c_k + \frac{\varpi}{\Delta}) + 2\delta e_{k2} (c_k e_{k2} + \frac{\varpi}{\Delta}) \right\} + c_k \delta^2 e_{k2}^2 [\varepsilon_k^2 (4l\rho^2 + 4\rho^2 - l^2 - 6\rho^4 - 1) - l^2] \right\} \\
&+ \varpi \delta e_{k2}^2 \left\{ \Delta c_k (2\varepsilon_k + 2 - \varepsilon_k \rho^2) + \gamma_k \right\} + \gamma_k e_{k3} \left( \frac{\sigma^2}{\tau p} + \gamma_k + \varpi \right) + 2 \frac{M^2}{N^2} |f_k(\Phi)|^2 \Delta^2 c_k \delta \varepsilon_k \rho^2 \left\{ c_k (1 + e_{k2}) [\delta \varepsilon_k (2\rho^2 - 1 - l) e_{k2} + e_{k1}] + \frac{\varpi}{\Delta} e_{k1} e_{k2} \right\} \\
&+ \frac{M^2}{N^2} \Delta^2 c_k^2 \delta^2 \varepsilon_k^2 e_{k2} (l - \rho^2) \left\{ |F_{kk}(\Phi)|^2 e_{k2} (l - \rho^2) + 2 \text{Re} \left\{ f_k(\Phi)^2 F_{kk}^H \right\} \rho^2 \right\} + \frac{M^2}{N^2} \Delta^2 c_k^2 \delta^2 e_{k2}^2 l^2 \left| \mathbf{a}_N^T \Phi^H \Phi^H \mathbf{a}_N \right|^2 \\
&+ \frac{M}{N} |f_k(\Phi)|^2 \Delta c_k \delta \varepsilon_k \rho^2 \left\{ \Delta c_k (\varepsilon_k + 1) (e_{k2} + 1) + \gamma_k + \left( \varpi + \frac{\sigma^2}{\tau p} + \gamma_k \right) e_{k2}^2 \right\} + \frac{M}{N} \Delta^2 c_k^2 \left\{ (2\varepsilon_k + 1) (2\delta e_{k2}^2 + e_{k3}) - 4\delta \varepsilon_k \rho^2 e_{k2}^2 \right\} \\
&+ M \left\{ \Delta c_k \left\{ \Delta c_k (\varepsilon_k + 1) + 2\gamma_k + \frac{\sigma^2}{\tau p} \right\} \left\{ (\delta e_{k2}^2 + e_{k3}) (\varepsilon_k + 1) - \delta \varepsilon_k \rho^2 e_{k2}^2 \right\} + \Delta c_k (\varepsilon_k + 1) \left\{ \Delta c_k \delta e_{k2}^2 [\varepsilon_k (1-\rho^2) + 1] + \varpi e_{k3} \right\} \right. \\
&+ \left. \frac{M^2}{N} |f_k(\Phi)|^2 \Delta^2 c_k \delta^2 \varepsilon_k \rho^2 \left\{ c_k \left\{ (e_{k2}^2 - 1)^2 + 2e_{k1} + \varepsilon_k (1-\rho^2) (e_{k2}^2 + 1) \right\} + \frac{\varpi}{\Delta} e_{k2}^2 \right\} \right\}. \quad (116)
\end{aligned}$$

- [3] C. Pan et al., "Multicell MIMO communications relying on intelligent reflecting surfaces," *IEEE Trans. Wireless Commun.*, vol. 19, no. 8, pp. 5218–5233, Aug. 2020.
- [4] C. Huang et al., "Holographic MIMO surfaces for 6G wireless networks: Opportunities, challenges, and trends," *IEEE Wireless Commun.*, vol. 27, no. 5, pp. 118–125, Oct. 2020.
- [5] L. Sanguinetti, E. Björnson, and J. Hoydis, "Toward massive MIMO 2.0: Understanding spatial correlation, interference suppression, and pilot contamination," *IEEE Trans. Commun.*, vol. 68, no. 1, pp. 232–257, Jan. 2020.
- [6] Z. Peng, X. Chen, W. Xu, C. Pan, L.-C. Wang, and L. Hanzo, "Analysis and optimization of massive access to the IoT relying on multi-pair two-way massive MIMO relay systems," *IEEE Trans. Commun.*, vol. 69, no. 7, pp. 4585–4598, Jul. 2021.
- [7] M.-H. T. Nguyen, E. Garcia-Palacios, T. Do-Duy, O. A. Dobre, and T. Q. Duong, "UAV-aided aerial reconfigurable intelligent surface communications with massive MIMO system," *IEEE Trans. Cogn. Commun. Netw.*, vol. 8, no. 4, pp. 1828–1838, Dec. 2022.
- [8] P. Wang, J. Fang, L. Dai, and H. Li, "Joint transceiver and large intelligent surface design for massive MIMO mmWave systems," *IEEE Trans. Wireless Commun.*, vol. 20, no. 2, pp. 1052–1064, Feb. 2021.
- [9] J. He, K. Yu, Y. Shi, Y. Zhou, W. Chen, and K. B. Letaief, "Reconfigurable intelligent surface assisted massive MIMO with antenna selection," *IEEE Trans. Wireless Commun.*, vol. 21, no. 7, pp. 4769–4783, Jul. 2022.
- [10] E. Björnson, Ö. Özdogan, and E. G. Larsson, "Intelligent reflecting surface versus decode-and-forward: How large surfaces are needed to beat relaying?" *IEEE Wireless Commun. Lett.*, vol. 9, no. 2, pp. 244–248, Feb. 2020.
- [11] Y. Han, W. Tang, S. Jin, C.-K. Wen, and X. Ma, "Large intelligent surface-assisted wireless communication exploiting statistical CSI," *IEEE Trans. Veh. Technol.*, vol. 68, no. 8, pp. 8238–8242, Aug. 2019.
- [12] M.-M. Zhao, Q. Wu, M.-J. Zhao, and R. Zhang, "Intelligent reflecting surface enhanced wireless networks: Two-timescale beamforming optimization," *IEEE Trans. Wireless Commun.*, vol. 20, no. 1, pp. 2–17, Jan. 2021.
- [13] A. Abrardo, D. Dardari, and M. Di Renzo, "Intelligent reflecting surfaces: Sum-rate optimization based on statistical position information," *IEEE Trans. Commun.*, vol. 69, no. 10, pp. 7121–7136, Oct. 2021.
- [14] C. Hu, L. Dai, S. Han, and X. Wang, "Two-timescale channel estimation for reconfigurable intelligent surface aided wireless communications," *IEEE Trans. Commun.*, vol. 69, no. 11, pp. 7736–7747, Nov. 2021.
- [15] K. Zhi, C. Pan, H. Ren, and K. Wang, "Power scaling law analysis and phase shift optimization of RIS-aided massive MIMO systems with statistical CSI," *IEEE Trans. Commun.*, vol. 70, no. 5, pp. 3558–3574, May. 2022.
- [16] K. Zhi et al., "Two-timescale design for reconfigurable intelligent surface-aided massive MIMO systems with imperfect CSI," *IEEE Trans. Inf. Theory*, vol. 69, no. 5, pp. 3001–3033, May. 2023.
- [17] M. Najafi, V. Jamali, R. Schober, and H. V. Poor, "Physics-based modeling and scalable optimization of large intelligent reflecting surfaces," *IEEE Trans. Commun.*, vol. 69, no. 4, pp. 2673–2691, Apr. 2021.
- [18] Z. Zhang et al., "Active RIS vs. passive RIS: Which will prevail in 6G?" *IEEE Trans. Commun.*, vol. 71, no. 3, pp. 1707–1725, Mar. 2023.
- [19] L. Dong, H.-M. Wang, and J. Bai, "Active reconfigurable intelligent surface aided secure transmission," *IEEE Trans. Veh. Technol.*, vol. 71, no. 2, pp. 2181–2186, Feb. 2022.
- [20] K. Zhi, C. Pan, H. Ren, K. K. Chai, and M. Elkashlan, "Active RIS versus passive RIS: Which is superior with the same power budget?" *IEEE Commun. Lett.*, vol. 26, no. 5, pp. 1150–1154, May. 2022.
- [21] Y. Ma, M. Li, Y. Liu, Q. Wu, and Q. Liu, "Active reconfigurable intelligent surface for energy efficiency in MU-MISO systems," *IEEE Trans. Veh. Technol.*, vol. 72, no. 3, pp. 4103–4107, Mar. 2023.
- [22] Q. Li, M. El-Hajjar, I. Hemadeh, D. Jagyasi, A. Shojafard, and L. Hanzo, "Performance analysis of active RIS-aided systems in the

- face of imperfect CSI and phase shift noise," *IEEE Trans. Veh. Technol.*, vol. 72, no. 6, pp. 8140–8145, Jun. 2023.
- [23] Z. Peng, X. Liu, C. Pan, L. Li, and J. Wang, "Multi-pair D2D communications aided by an active RIS over spatially correlated channels with phase noise," *IEEE Wireless Commun. Lett.*, vol. 11, no. 10, pp. 2090–2094, Oct. 2022.
- [24] M.-A. Badiu and J. P. Coon, "Communication through a large reflecting surface with phase errors," *IEEE Wireless Commun. Lett.*, vol. 9, no. 2, pp. 184–188, Feb. 2020.
- [25] A. Papazafeiropoulos, C. Pan, P. Kourtessis, S. Chatzinotas, and J. M. Senior, "Intelligent reflecting surface-assisted MU-MISO systems with imperfect hardware: Channel estimation and beamforming design," *IEEE Trans. Wireless Commun.*, vol. 21, no. 3, pp. 2077–2092, Mar. 2022.
- [26] J.-F. Bousquet, S. Magierowski, and G. G. Messier, "A 4-GHz active scatterer in 130-nm CMOS for phase sweep amplify-and-forward," *IEEE Trans. Circuits Syst. I, Reg. Papers*, vol. 59, no. 3, pp. 529–540, Mar. 2012.
- [27] E. Björnson, J. Hoydis, and L. Sanguinetti, "Massive MIMO networks: Spectral, energy, and hardware efficiency," *Found. Trends Signal Process.*, vol. 11, no. 3-4, pp. 154–655, Nov. 2017.
- [28] B. Hassibi and B. M. Hochwald, "How much training is needed in multiple-antenna wireless links?" *IEEE Trans. Inf. Theory*, vol. 49, no. 4, pp. 951–963, Apr. 2003.
- [29] Z. Peng, X. Chen, C. Pan, M. ElKashlan, and J. Wang, "Performance analysis and optimization for RIS-assisted multi-user massive MIMO systems with imperfect hardware," *IEEE Trans. Veh. Technol.*, vol. 71, no. 11, pp. 11 786–11 802, Nov. 2022.
- [30] R. Long, Y.-C. Liang, Y. Pei, and E. G. Larsson, "Active reconfigurable intelligent surface-aided wireless communications," *IEEE Trans. Wireless Commun.*, vol. 20, no. 8, pp. 4962–4975, Aug. 2021.
- [31] Q. Wu, S. Zhang, B. Zheng, C. You, and R. Zhang, "Intelligent reflecting surface-aided wireless communications: A tutorial," *IEEE Trans. Commun.*, vol. 69, no. 5, pp. 3313–3351, May. 2021.
- [32] B. Zheng, C. You, and R. Zhang, "Double-IRS assisted multi-user MIMO: Cooperative passive beamforming design," *IEEE Trans. Wireless Commun.*, vol. 20, no. 7, pp. 4513–4526, Jul. 2021.
- [33] S. M. Kay, *Fundamentals of Statistical Signal Processing*. Upper Saddle River, NJ, USA: Prentice-Hall, 1993.